

2022

A Combinatorial 5-HTR Expression Pattern within the Ventral Projection Neurons of the *D. melanogaster* Olfactory Circuit.

Mohd Freezely Ezzani Bin Mazri
mfm0003@mix.wvu.edu

Follow this and additional works at: <https://researchrepository.wvu.edu/etd>



Part of the [Biology Commons](#), and the [Neuroscience and Neurobiology Commons](#)

Recommended Citation

Mazri, Mohd Freezely Ezzani Bin, "A Combinatorial 5-HTR Expression Pattern within the Ventral Projection Neurons of the *D. melanogaster* Olfactory Circuit." (2022). *Graduate Theses, Dissertations, and Problem Reports*. 11381.

<https://researchrepository.wvu.edu/etd/11381>

This Thesis is protected by copyright and/or related rights. It has been brought to you by the The Research Repository @ WVU with permission from the rights-holder(s). You are free to use this Thesis in any way that is permitted by the copyright and related rights legislation that applies to your use. For other uses you must obtain permission from the rights-holder(s) directly, unless additional rights are indicated by a Creative Commons license in the record and/ or on the work itself. This Thesis has been accepted for inclusion in WVU Graduate Theses, Dissertations, and Problem Reports collection by an authorized administrator of The Research Repository @ WVU. For more information, please contact researchrepository@mail.wvu.edu.

**A Combinatorial 5-HT_{1A} Expression Pattern within the Ventral Projection Neurons of the
D. melanogaster Olfactory Circuit.**

Mohd Freezely Ezzani Bin Mazri

**Thesis submitted
to the Eberly College of Arts and Science
At West Virginia University**

in partial fulfillment of the requirements

for the degree of

Master of Science

In Biology

Andrew M. Dacks, Ph.D., Chair

Kevin C. Daly, Ph.D.

Eric J. Horstick, Ph.D.

Department of Biology

Morgantown, WV

2022

**Keywords: Neuromodulation, Serotonin, Olfaction, Ventral Projection Neurons,
*Drosophila***

Copyright 2022 Mohd F. Mazri

Abstract

A Combinatorial 5-HT_{1A} Expression Pattern within the Ventral Projection Neurons of the *Drosophila* Olfactory Circuit.

Mohd Freezely Ezzani Bin Mazri

Neuromodulation allows neurons within a circuit to respond to stimuli from the environment according to the correct ecological value, context, and internal state of the animal. Serotonin (5-HT) is a neuromodulator that can generate different outcomes based on its target's serotonin receptor (5-HT_{1A}) expression by affecting secondary messenger cascades. Within the *Drosophila* olfactory system, ventral projection neurons (vPN) express all five insect 5-HT_{1A} that project into two olfactory processing regions, the antennal lobe (AL) and the lateral horn (LH). The significance of this 5-HT_{1A} expression is unknown. In this study, I theorized the patterns of 5-HT_{1A} expression of vPNs. I took advantage of two transgenic approaches, one that enabled me to use fluorescent proteins to observe two populations of vPNs and determine co-expression patterns while another that allows me to stochastically express individual vPNs that express a given 5-HT_{1A}. I categorized the vPN population into two types, the excitatory ventral projections (e-vPN) which respond to both attractive and aversive glomeruli, and inhibitory ventral projection neurons (i-vPN) which respond to attractive glomeruli. Through these approaches, I found 5-HT_{1A} co-expression in both vPN populations, different innervation patterns of 5-HT_{1A} expressing vPNs in both olfactory processes, and two populations of i-vPN neurons that express distinct 5-HT_{1A} expression and morphology patterns. This study helps us understand 5-HT modulation of a diverse 5-HT_{1A} population and lays a foundation to study the functional and behavioral roles of i-vPN subpopulations in odor-guided behavior.

ACKNOWLEDGMENTS

First and foremost, I would like thank and praise to The Almighty, for sustaining me and blessing me with good health and a strong mind to undergo this journey to be a better person in life. Next, I would like to thank my mother for her continuous support, prayers and good advice as well as my father who served as an inspiration for me to pursue my dreams in higher education. Next, I would like to thank my principal investigator, professor, and role model Dr. Andrew Dacks for introducing me into the world of neuroscience and allowing me to be a part of his journey to understand more about the mysteries of the brain. I would like to thank him for believing in me, sharing his wisdom, and having great patience to allow me to grow in this discipline. May you be blessed with more goodness in this word and the next.

Next, I would also like to thank all my teachers and professors, from college professors to friends, who have planted in me a great curiosity for knowledge, wisdom, and good character. My journey in my Masters could not have been successful without the company of my lab colleagues, peers from my local mosque, and close friends. Thank you for always having the time to listen, share a good word, and support during both the easy and challenging times.

To all my family, teachers, and friends, may your hands always be filled with bounty, your paths be full of goodness and your burdens be removed.

TABLE OF CONTENTS

ABSTRACT.....	ii
ACKNOWLEDGEMENTS.....	iii
TABLE OF CONTENTS.....	iv
LIST OF FIGURES.....	v
LIST OF TABLES.....	vi
LIST OF ABBREVIATIONS.....	vii
CHAPTER 1: Introduction.....	1
CHAPTER 2: Determining the 5-HTR Expression and Morphological Innervations of vPNs that Express a Given 5-HTR.....	8
I. Abstract.....	8
II. Introduction.....	9
III. Methods and Materials.....	11
IV. Results.....	26
V. Discussion.....	33
VI. List of Figures.....	39
CHAPTER 3: Future Directions.....	51
REFERENCES.....	56

LIST OF FIGURES

Figure 1. Morphology of vPN entering the AL through multiple AL fascicles.....	39
Figure 2. Schematic diagram of predicted 5-HTR expression within the vPN population.....	40
Figure 3. i-vPN 5-HTR co-expression within two 5-HTR populations.....	41
Figure 4. e-vPN 5-HTR co-expression within two 5-HTR populations.....	42
Figure 5. Representation of vPN glomerular innervation expressing each 5-HTR using MCFO.....	43
Figure 6. Glomerular heat map of percent positive innervation of each 5-HTR expressing vPN.....	44
Figure 7. Various vPN MCFO expressions for each 5-HTR subtype.....	45
Figure 8. Two i-vPN subpopulations expressing distinct innervation patterns in the AL and LH.....	46
Figure 9. 5-HT expression of the R24H08-LexA i-vPN subpopulation.....	47
Figure 10. 5-HT expression of the R86G06-LexA i-vPN subpopulation.....	48
Figure 11. Graph representation of 5-HTR expression between two i-vPN subpopulations.....	49
Figure 12. Two behavioral assays used to understand the consequence of R86G06-Gal4 i-vPN 5-HT7 knockdown on odor-guided behavior.....	50

LIST OF TABLES

Table 1. Genotypes used in Chapter 2, Aim 2.....	15
Table 2. Antibodies used for immunocytochemistry.....	16
Table 3. Predicted Odor Valence of Analyzed Glomeruli	17

LIST OF ABBREVIATIONS

5-HT	Serotonin
5-HTR	Serotonin Receptor
OSN	Olfactory Sensory Neuron
LN	Local interneuron
vPN	Ventral projection neuron
vIPr	Ventrolateral protocerebrum neuron
vPN	Ventral Projection Neuron
e-VPN	Excitatory ventral projection neuron
i-vPN	Inhibitory ventral projection neuron
CSDn	Contralaterally projecting, serotonin-immunoreactive, deutocerebral neuron
mIALT	Mediolateral antennal lobe tract
mALT	Medial antennal lobe tract
AL	Antennal lobe
MB	Mushroom body
GPCR	G-protein coupled receptor
MCFO	MultiColor FlpOut
GFP	Green fluorescent protein
RFP	Red fluorescent protein
RNAi	Ribonucleic acid interference

Chapter 1: Introduction

The environment provides many sources of stimuli that are detected by our sensory systems. This information is collected, refined through multiple layers of processing, and eventually converted into a motor action. In addition to encoding the stimulus itself, sensory systems must also factor in the contexts in which the stimulus is found or the internal state of the animal. In the context of olfaction, an odor of a single food source can represent a simple signal. In reality, this stimulus is further complicated by the combination of odor concentration, negative valences in the source (aversive odors from mold or predatory pheromones) as well as the internal states (i.e., satiety, arousal, sleep) of the animal. There need to be a mechanism that enables behavioral flexibility to allow the animal to process odor information effectively as well as safeguard itself from danger, from mold, bacteria, and predators found near a food source.

Neuromodulation is a strategy that allows behavioral flexibility by altering the physiological properties and synaptic strength of a signal neuron within a network (Reviewed in Bargmann 2012; Marder 2012; Marder et al. 2014). It is governed by two components; the modulatory ligand secreted by a modulatory neuron and its receptor that accepts the ligand to affect the neuron's downstream signaling cascade. By increasing or decreasing a secondary messenger cascade, the neuromodulator changes the physiological and synaptic properties of a neuron. In addition, neuromodulators target neurons through direct and indirect pathways (Eid et al. 2013). Even if a neuron does not express a neuromodulatory receptor, it can still be affected by its partner that expresses a modulatory receptor. Neuromodulation gives a neuron and a circuit extra capability to change its synaptic environment, allowing it to respond effectively to the external stimuli in the environment.

Serotonin (5-hydroxytryptophan, 5-HT) is a commonly expressed neuromodulator across both vertebrates and invertebrates. 5-HT has a role in regulating appetite, arousal states, and learning, showing its multi-functional influence across different neuronal circuits (Johnson et al. 2009; Becnel et al. 2011; Monti 2011; Renner et al. 2012; Gasque et al. 2013; Luo et al. 2016; Huser et al. 2017; Ren et al. 2018). This neuromodulator is derived from three main sources; the gut (90% of 5-HT), the blood (8% of 5-HT), and the brain (2% of 5-HT) (Berger et al. 2009). Sensory systems are mostly influenced by brain-derived serotonin; therefore, it is important to understand the effects of releasing this neuromodulator.

Serotonin receptors (5-HTR) are mostly G-protein coupled receptors (GPCR) that when bound by serotonin activate a signaling cascade (Nichols and Nichols 2008). Within vertebrates, there are a total of seven 5-HT subtypes while invertebrates have at least three (5-HT1, 5-HT2, and 5-HT7) (Reviewed in Sizemore et al. 2020). These 5-HTR subtypes can be distinguished by the signaling pathway to which they couple and their binding affinity to serotonin. For example, insects express five types of 5-HTR; 5-HT1A, 1B, 2A, 2B, and 7 (Saudou et al. 1992). 5-HT1R (5-HT1A and 1B subtypes) are negatively coupled to adenylyl cyclase to inhibit the PKA pathways. In addition, 5-HT7 is positively coupled to the adenylyl

cyclase pathway causing an excitatory effect on the signaling pathway. The PKA pathways interact with many intracellular targets which in turn affect the membrane excitability and changes in gene expression (Nichols and Nichols 2008; Tierney 2018). On the other hand, 5-HT₂ (5-HT_{2A} and 2B subtypes) couple positively to the IP₃ pathway which results in the release of intracellular Ca²⁺, affecting more structural changes within the cell (Nichols and Nichols 2008; Tierney 2018). The binding affinities of serotonin receptors differ from one another. Out of the five 5-HTR subtypes in insects (5-HT_{1A}, 1B, 2A, 2B, and 7), 5-HT₇ has the highest binding affinity for serotonin, followed by 5-HT_{2A}, 2B, 1B, and 1A being the least sensitive (Gasque et al. 2013). This shows that the concentration of 5-HT being released can determine how neurons are affected within a circuit depending on the sensitivity of the 5-HTRs being expressed by a circuit component.

Furthermore, serotonin receptors can form interactions with each other through dimerization (reviewed in Herrick-Davis 2013; Maroteaux et al. 2019). Reports describe 5-HT_{1A}-5-HT₇ heterodimers differ in their intracellular signaling targets. 5-HT_{1A} heterodimers are coupled with pertussis-toxin (PTX)-sensitive GPCR, when activated reduced G protein-coupled inwardly rectifying potassium (GIRK) conductance without affecting its 5-HT₇ heterodimer which increases ERK1/2 phosphorylation (Renner et al. 2012). GIRK channel activation causes an influx of K⁺ into the cell which leads to neuronal-self inhibition (Lüscher and Slesinger 2010). GIRK can also be regulated by multiple pathways, including the PKA and PKC pathways which are usually coupled with 5-HT. Therefore, a reduction in GIRK activity by 5-HT_{1A} would increase cellular and synaptic activity in a cell (Renner et al. 2012). ERK1/2 phosphorylation activation promotes cellular activity through the regulation of cellular processes such as cell survival, differentiation, and transcription (Roskoski 2012).

Dimerization of neuromodulatory receptors allows a cell to obtain access to different signaling pathways and differential effects, whether inhibitory or excitatory when the ligand is present. Dimerization occurs as a form of quality control as the protein is being trafficked from the endoplasmic reticulum (ER) to the plasma membrane (Herrick-Davis 2013). This quality control, also known as proteostasis, determines whether newly synthesized proteins meet the standard and structure to function normally (Araki and Nagata 2011). Responses towards a dimer vary depending on accessibility to the binding site of the protein. When a homodimer is available for ligand binding, only one activation of a site is sufficient to activate the signal cascade. An increased response would occur if both sites are ligand bounded. Besides that, heterodimerization allows for the activation of two different dimer types. This causes differences in activation based on what ligands and concentrations of ligands are present in the environment. Dimerization can be differentiated by receptor co-expression as dimers have the potential to block their partner through conformational change while co-expressed receptors are a subunit of their own (Herrick-Davis 2013).

There could be possibilities of neurons having localized receptor expression within different processes of their structure. Past research suggests that mRNA of a glycine receptor could be differentiated in the somatic versus the dendritic area (Racca et al. 1998; Kiebler and DesGroseillers 2000). Such localization allows for easier access for translation near the dendritic zones. However, I didn't find any research on the localization of different modulatory receptors, having such an expression can lead to different neuromodulatory effects on a region based on the coupling of the receptor. For example, a neuron could have different modulatory activities in its dendritic, somatic, and axon sites by the same neuron by expressing different 5-HTR subtypes within each region. Taken together, 5-HTRs can cause long-term effects that promote cellular enhancement or inhibition. This ability allows neurons to have more flexibility in coding. Plus, with 5-HTRs capable of forming dimer combinations, different pathways of activation and inhibition can be accessed to respond to changes in cellular activity. My thesis aims to characterize the organizational patterns of 5-HTR expression within a population of neurons knowing the various ways a 5-HTR could be expressed in a population.

Drosophila melanogaster serves as an excellent model to answer questions about the role of 5-HTR expression with a neural circuit. The *Drosophila* model fulfills three key elements for studying the neuromodulation of circuits. *Drosophila* has 1) a numerically reduced olfactory system, having fewer neurons and 5-HTR types compared to vertebrates (Reviewed in Vosshall and Stocker 2007), 2) an established basic framework of its sensory circuits (Jefferis et al. 2007; Liang and Luo 2010; Ito et al. 2014), and 3) possessing powerful connectome datasets (Zheng et al. 2018; Bates et al. 2020; Scheffer et al. 2020; Phelps et al. 2021), and genetic tools which allow for better access and comparative analysis of the neurons of interest (Pfeiffer et al. 2010; Jenett et al. 2012; Gnerer et al. 2015).

The olfactory circuit of *Drosophila melanogaster* is a well-established sensory system that could be used as a reference to understand its mammalian counterpart (Wilson 2013; Grabe and Sachse 2018). Olfactory processing begins when chemical ligands bind to chemosensory receptor proteins expressed by olfactory sensory neurons (OSN) found in the antennae and maxillary palps. Upon ligand binding, a signaling cascade causes the OSN to depolarize, transducing this chemical signal into an electrical signal which gets transmitted into the antennal lobe (AL), the next order of information processing. Each OSN projects to specific neuropils within the AL called glomeruli. The AL contains about 50 odor-responsive glomeruli and 7 additional glomeruli that respond to other physical glomeruli including humidity, cold, and heat which refine and integrate information before being relayed to higher processing regions (Laissue et al. 1999; Wong et al. 2002; Task et al. 2022). The principal neurons that facilitate these activities are projection neurons (PNs) which relay information from one region to another and local interneurons (LNs) which fine-tune the odor-coding space. Processed olfactory information is relayed to two regions, the mushroom body (MB) which plays a role in associative learning, and the lateral horn (LH) which influences innate behavioral responses (Aso et al. 2014; Dolan et al. 2019; Das Chakraborty and Sachse 2021). My thesis focuses on sensory processing occurring within the first and second-order

information processing stages, the AL and LH, and the projection neurons that relays the information between these regions. I will describe the roles of these components and how serotonergic modulation can affect my neurons of interest.

Olfactory coding has been well studied across multiple processing stages in the circuit (Reviewed in Wilson 2013; Grabe et al. 2016; Grabe and Sachse 2018). Olfactory processing in the AL begins in a glomerulus when an OSN synapse onto a PN. OSNs are cholinergic and form strong synaptic connections with PNs, thus an OSN spike can quickly trigger PN activity. Within a glomerulus, individual LNs arborize within many neuropils, providing lateral excitation or inhibition. This allows LNs to change the input from multiple glomeruli and fine-tune the neural activity of other glomeruli to influence odor processing based on the ongoing activity within the network (Wilson 2013; Grabe and Sachse 2018). For example, when odors are present, LNs serve to suppress the spontaneous activity of glomeruli not targeted by the odor, promoting the activation of selected PNs (Olsen et al. 2007; Olsen and Wilson 2008; Olsen et al. 2010).

In other situations, the final valence context of a given odor can switch when an odor is sampled together with another odor or detected at a high concentration. For example, with an introduction of an odor from a toxic source, the synaptic cell activity needs to change to cause an aversive behavioral response. There are specific labeled line systems that trigger an overriding behavioral response, for example, the aversive odor geosmin (Stensmyr 2012). However, toxicity could also arise from the attractive odor that is present in higher concentrations, such as acetic acid (Devineni et al. 2019). Taken together, OSN, LNs, and PNs are connected strongly together to ensure rapid and flexible communication to relay the message to the next order of processing.

After the information is processed in the AL, PNs carry information into two regions, the mushroom body (MB) and the lateral horn (LH). The MB is commonly associated with learned behavior while the LH mediates innate behavior (Heisenberg 2003; Aso et al. 2014; Schultzhaus et al. 2017; Bates et al. 2020; Das Chakraborty and Sachse 2021; Devineni and Scaplen 2022; Khallaf and Knaden 2022). PNs travel to these regions through specific tracts; 1) the mALT innervates the MB before the LH and 2) the mIALT which directly terminates in the LH. It has been hypothesized that mALT PNs are cholinergic while mIALT PNs are GABAergic (Bates et al. 2020), although this needs further exploration. PNs also form axo-axonic connections with each other in these higher processing regions, as well as gap junctions in the AL, adding a layer of complexity of communication between these two neuropil regions (Wang et al. 2014; Shimizu and Stopfer 2017; Bates et al. 2020).

The LH has been increasingly studied within the last decade (reviewed in Das Chakraborty and Sachse 2021). The LH does not contain glomeruli that organize coding information based on the chemical structure of the odorant, instead PNs project the neuropil in specific zones that encode hedonic valence and odor intensity (Jefferis et al. 2007, Strutz et al. 2014). PNs synapse upon lateral horn neurons (LHN), consisting of both LH output neurons (LHON) with LH local neurons (LHLN) fine-tuning LHN cellular

activity (Dolan et al. 2019; Frechter et al. 2019; Das Chakraborty et al. 2022). In contrast, lateral horn neurons (LHNs) differ in the way that they tune integrated information from multiple glomeruli carried by the PNs (reviewed in Jeanne et al. 2018; Frechter et al. 2019; Bates et al. 2020; Das Chakraborty and Sachse 2021). PNs with similar odor encoding glomeruli converge to similar regions in the LH (Jeanne et al. 2018). These sister PNs, converge to the same LHN, resulting in stronger odor detection performance. Singular PN however would form more synaptic connections with their LHN targets equivalent to that of a sister-PN (Jeanne et al. 2018). Different tuning capabilities suggest that LHN activity allows the animal to distinguish odors based on behavioral significance, hedonic valence, and innate predisposition to an odor (Jefferis et al. 2007; Strutz et al. 2014; Frechter et al. 2019; Das Chakraborty et al. 2022).

The outcome of the LH output results in a motor behavior based on the targeted regions. LHNs interactions are complex since high-order input receives broad signals from other regions of the brain such as the visual, mechanosensory, and gustatory centers (Dolan et al. 2019). Although some stereotypical innervations of PNs could be observed within the region, more information is needed to classify each role of LHNs in the population. While we know a lot about the input zones of the different ePNs (Marin et al. 2002; Jefferis et al. 2007; Bates et al. 2020), there is a large diversity of LHNs. The estimated population of LHN is about ~560 LHLN and ~830 LHON with more than 167 core cell types (Frechter et al. 2019). Such a large population suggests that LHNs process stereotype odor categories as well as different aspects of odor behavior (Frechter et al. 2019). Interestingly, LHONs were suggested to relay to a final layer of information processing in the superior lateral protocerebrum (SLP) as there are no currently identified LHONs projecting to the ventral nerve cord (VNC) (Dolan et al. 2019). Taken together, the lateral horn contains many cell types with multiple roles that collect and integrate input from multiple sensory neuropil which are further processed at higher order brain regions before being processed into motor behavior.

PNs can be classified based on their morphology and neurotransmitter content. There are two types of PN morphologies within the AL, uniglomerular PNs (uPNs) and multiglomerular PNs (mPN). uPNs are more specific because they received input from only one OSN type while mPNs receive input from multiple OSNs (Parnas et al. 2013; Wang et al. 2014; Shimizu and Stopfer 2017). This is important to tackle the many factors that influence the odor space such as odor type, concentration, hedonic valence, animal's behavioral state, and ecological relevance (Vosshall 2000; Knaden et al. 2012; Stensmyr et al. 2012; Ziegler et al. 2013; Strutz et al. 2014; Vogt et al. 2021). Since PNs are very sensitive to OSN signals, having uniglomerular connections allow for specific odor coding while multiglomerular innervation allows broadly tuning of odor coding (Wang et al. 2014). For example, the aversive chemical geosmin found in mold is detected by a uPN that only innervates the DA2 glomerulus. A low concentration (10^{-6}) is sufficient to stimulate negative feeding and egg-laying response (Stensmyr et al. 2012). Additionally, uPNs can form synapses with mPNs to respond to a context-based behavior.

For example, i-vPN lines that inhibit LH responses also excite ePNs through chemical synapses which then output to the LH (Parnas et al. 2013). In terms of neurotransmitter content, most uPNs are cholinergic (n=127) with some GABAergic (n=25) while GABAergic PN classes are split between the two types (Ach mPN = 73 and GABA mPN = 71) (Bates et al. 2020). Furthermore, PN classes can be segregated based on the location of their soma into one of 3 clusters around the AL (Ito et al. 2014); anterodorsal projection neurons (adPN), lateral projection neurons (latPN), and ventral projection neurons (vPNs) (Jefferis et al. 2007). Another paper include a fourth neuron cluster, the lateroventral PNs (lv-PNs) (Sakuma et al. 2014). In totality, the known PN population is estimated to be around 347 neurons but there is a likelihood of more neurons in the population.

As previously mentioned, a sole source of serotonin is released within the *Drosophila* AL and LH by neurons known as the “contralaterally-projecting, serotonin-immunoreactive deutocerebral neurons” CSDns (Roy et al. 2007; Coates et al. 2017). The CSDns can provide output to the PNs as well as receive input from presynaptic PN targets. Within the AL, CSDn primarily synapses onto LNs, uPNs, and mALT mPNs but has few synapses mlALT mPNs in the LH (Coates et al. 2020). These synaptic connections are heterogeneous, indicating that 5-HT could lead to different effects depending of 5-HTR expression across the AL and LH.

Ventral projection neurons (vPNs) are a group of cholinergic or GABAergic neurons located in the ventral cluster of the AL. vPNs are multiglomerular, entering through the AL via the AL fascicle. Based on neurotransmitter content, cholinergic lv-PNs (e-vPNs) are hypothesized to project to the MB body and LH through the mALT while GABAergic vPN (i-vPNs) project directly to the LH via mlALT (Okada et al. 2009; Tanaka et al. 2012). vPNs studies mostly involve two Gal-4 lines, GH146-Gal4 and MZ699-Gal4 (Yasuyama et al. 2003; Jefferis et al. 2007; Lai et al. 2008; Liang et al. 2013; Sizemore and Dacks 2016). Out of the total of 51 vPNs in MZ699-Gal4, only 36 vPNs are GABAergic (Sizemore and Dacks 2016). Since we know that vPNs are non-glutamnergic mPNs, the 71 GABAergic mPN and a proportion of the 73 cholinergic mPN may belong to the vPN cluster (Bates et al. 2020).

In terms of serotonergic receptor expression, vPNs are unique because as a population they express all insect 5-HTRs (1A, 1B, 2A, 2B, and 7) in contrast to the other neural class and clusters which express between one to three types (Sizemore and Dacks 2016). The consequence behind this diversity is unknown. Since each receptor targets different secondary messenger pathways and has different binding affinities for 5-HT, could expressing all 5-HTRs provide a new avenue to modulate odor-based stimuli within the olfactory system? We would also like to know if there is a pattern of 5-HTR expression or bias to specific odor types and valence. Furthermore, how would a disruption in 5-HTR expression by vPNs affect odor-guided behavior? My thesis aims to answer these questions in four ways; 1) Using immunocytochemistry and transgenics to characterize the pattern of 5-HTR co-expression within the vPN cluster, 2) Using immunochemistry and transgenics to identify individual vPNs at random that express each 5-HTR to determine the olfactory regions they innervate, 3) Using immunocytochemistry and

transgenics to identify subpopulations of a vPN type with distinct patterns of 5-HTR expression and 4) Study the effects of vPN 5-HTR receptor knockdown and its effect on odor-guided behavior. Answering these questions would provide an anatomical outline for searching candidate vPNs in the connectome dataset and also open physiology and behavioral questions to understand the role and effect of 5-HT modulation within a diverse population. It would also allow us to explore the ways 5-HT modulation could occur within different stages of olfactory coding, and how that could contribute to animal's behavior. We hope that this approach will help provide a framework for understanding neuromodulatory targets within this olfactory network.

Chapter 2: Determining the 5-HTR expression and morphological innervations of vPNs that express a given 5-HTR.

Abstract:

Sensory systems must be adapted to the ecological context and internal state of an animal to respond correctly to a stimulus. Neuromodulation provides a means to allow behavioral flexibility within neurons by targeting their modulatory receptors. Typically, neuromodulators target classes of neurons that express only one pattern of neuromodulatory receptors. However, there is a population that expresses all receptors of a given neuromodulator. The significance of this receptor expression diversity is unknown. Ventral projection neurons (vPNs) are a cell cluster found in the *Drosophila* olfactory system that expresses all 5-HTR types. This chapter aims to determine how vPNs express each 5-HTR type and what understanding we could take out from these expression patterns. I found that vPN to a degree co-express two receptor types in the population. I also found out that vPN expressing 5-HTR can be categorized into two groups, e-vPN (excitatory vPN), and i-vPN (inhibitory vPN) that go into overlapping regions in the glomeruli as well as respond to different odor valences. Finally, I found two subpopulations of i-vPNs that displayed different morphology, 5-HTR expression, and odor valence. Together, I showed the complexity of 5-HTR expression in a population that opens many routes for flexible odor processing.

Introduction:

Sensory systems rely on multiple strategies and mechanisms to respond to a variety of stimuli and contexts within an environment to efficiently provide the optimal response. Neuromodulation is an important strategy that allows a neuron to have multiple functional roles by altering its physiological state and synaptic connections (Bargmann 2012; Marder 2012; Marder et al. 2014). Serotonin (5-HT) is a well-studied neuromodulator in the nervous system, having a major role in regulating appetite, mood, and arousal responses (Nichols and Nichols 2008; Johnson et al. 2009; Huser et al. 2017; Ren et al. 2018; Devineni et al 2019.). Serotonin binds to several serotonin receptors (5-HTRs), a family of G-protein-coupled receptors (GPCR) that when liganded, activate a signaling cascade changing the activity of the cell. 5-HTR types are differentiated by the secondary messenger targets to which they couple and the manner of the coupling (positive or negative, with different latency and duration) (Nichols and Nichols 2008b). Therefore, a neuron could be differentially affected by expressing a given 5-HTR type they express. However, if neurons can have the ability to express multiple receptor types, how would 5-HT modulation affect its role? We know that 5-HTRs can form heterodimers, having the access to affecting multiple messenger pathways in a cell (Maroteaux et al. 2019). Finally, each 5-HTR type also has different binding affinities to 5-HT, allowing different concentrations of 5-HT to affect different 5-HTR expressing neurons (Gasque et al. 2013). To understand the implication of this effect, we would need to explore a serotonergic circuit that contains a neuron population that expresses each 5-HTR.

Drosophila is a suitable candidate for studying serotonergic modulation as it is a mathematically reduced model to understand sensory systems (Wilson 2013; Sizemore and Dacks 2016; Sizemore et al. 2020). This model organism contains plenty of publicly available datasets and transgenic tools which allow the observation and manipulation of a neuron population and its cellular contents (Pfeiffer et al. 2010; Jenett et al. 2012; Phelps et al. 2021). Insects express five types of 5-HTR receptors (5-HT1A, 5-HT1B, 5-HT2A, 5-HT2B, and 5-HT7), which affects behavior such as food-searching and courtship (Becnel et al. 2011; Gasque et al. 2013; Huser et al. 2017; Ganguly et al. 2020). The fly olfactory system is similarly organized to the vertebrate olfactory system (Liang and Luo 2010; Wilson 2013; Grabe and Sachse 2018). When an odorant is detected from the environment via olfactory sensory neurons (OSNs), the chemical signal is transduced into electrical output and carried into the glomeruli within the antennal lobe (AL, first-order olfactory region). OSN that express the same chemoreceptor proteins converge into the same glomeruli, and their activity is refined by local interneurons (LN). Through projection neurons (PNs), the processed information is relayed to the second-order olfactory regions, the mushroom body (MB), an associative learning center, and the lateral horn (LH), an innate behavior center (Aso et al. 2014; Das Chakraborty and Sachse 2021). This circuit is modulated by a pair of serotonergic neurons known as the “contralaterally projecting, serotonin-immunoreactive deutocerebral neurons” (CSDNs) (Dacks et al. 2006). These neurons project to multiple regions throughout the brain, including the olfactory circuit,

forming synaptic connections in both the AL and the LH (Dacks et al. 2009; Coates et al. 2020). Knowing this, 5-HT release can affect multiple regions of the brain.

The neuron populations surrounding the antennal lobe have been well characterized (Sizemore and Dacks 2016). Some populations express only one 5-HTR type such as OSNs which express only the 5-HT_{2B} receptors. Other populations express a combination of two or three types of 5-HTR like the peptidergic LNs expressing 5-HT_{1A}R and 5-HT₇R and the anterodorsal PN (adPNs) expressing 5-HT_{1A}R, 5-HT_{2B}R, and 5-HT₇R, respectively. In the most extreme case, ventral projection neurons express all five 5-HTRs. Currently, we don't know the significance behind multiple 5-HTRs being expressed within a population. Thus, vPNs may provide a good model for understanding the consequences of expressing multiple 5-HTRs by on neural population because they follow a specific morphology and project into two heavily studied olfactory regions, the AL and the LH.

The soma of vPNs is ventral to the AL which they enter via an AL fascicle (Sizemore and Dacks 2016; Bates et al. 2020). These neurons are generally multiglomerular in AL innervations and exit out the neuropil either of two paths; 1) the medio-antennal lobe tract (mALT) to the MB body and then LH or 2) the mediolateral antennal lobe tract (mlALT) directly to the LH (Bates et al. 2020; Coates et al. 2020). We know that there are ~144 detected vPNs (Bates et al. 2020) and vPNs that follow the mlALT are mostly GABAergic (Liang et al. 2013; Parnas et al. 2013; Strutz et al. 2014) while mALT vPN were thought to be cholinergic (Bates et al. 2020). Our goal is to understand how 5-HTR expression is organized within these two populations.

To understand how a population expresses all 5-HTR and understand its behavioral implications, we theorize to draw out the extremities of 5-HTR expression and the likelihood receptor expression pattern. Using available transcriptional reporters that rely on different binary expression systems, I examined the degree of overlap in the expression of 5-HTRs (Pfeiffer et al. 2010). Next, I sought to determine if vPNs expressing different 5-HTRs were more likely to innervate specific AL glomeruli or LH regions than others. Then, I used a stochastic labeling technique to sample a large number of brains to construct a representative glomerular map of vPNs expressing each 5-HTR. This allows us to construct a representative glomerular map of each 5-HTR expressing vPN to understand their common pattern in the AL, allowing us to predict the 5-HTR type based on glomeruli innervation. Next, I also identified driver lines expressing sparse vPNs subpopulations which also expresses different 5-HTRs and has little overlap in the AL and LH. Using one of these lines, I conducted two behavioral assays to understand the consequence of 5-HTR knockdown of a i-vPN subpopulation on odor-guided behavior. This combination of anatomical and behavioral approaches will help us understand more about how 5-HTR diversity operates within a population.

Material and Methods:

Genotypes used in Aim 1:

Aim 1.1 Figures: Multiple 5-HTR co-expression (Fig. 3, 4).

A) 5-HT7R-LexA co-expression analysis:

- 1) **Fig. 3B and 4B:** UAS-RFP, Aop-GFP;5HT1A/Cyo (BDSC 3229 stabled with MiMIC line from Herman Dierick, Gnerer et al. 2015) × w[*]; TI{2A-lexA::p65}5-HT2B[2A-D.lexA] (BDSC 84353)
- 2) **Fig. 3C and 4C:** UAS-RFP, Aop-GFP;5HT1B/Cyo (BDSC 3229 stabled with MiMIC line from Herman Dierick) × w[*]; TI{2A-lexA::p65}5-HT2B[2A-D.lexA] (BDSC 84354)
- 3) **Fig. 3D and 4E:** UAS-RFP, Aop-GFP;;5HT2B/TM3 (BDSC 3229, stabled with MiMIC line from Herman Dierick) × w[*]; TI{2A-lexA::p65}5-HT2B[2A-D.lexA] (BDSC 84354).
- 4) **Fig. 3E and 4D:** UAS-RFP, Aop-GFP;;5HT7/TM3 (BDSC 3229, stabled with MiMIC line from Herman Dierick) × w[*]; TI{2A-lexA::p65}5-HT2B[2A-D.lexA] (BDSC 84354).

B) 5-HT2BR-LexA co-expression analysis:

- 1) **Fig. 3F and 4F:** UAS-RFP, Aop-GFP;5HT1A/Cyo (BDSC 3229 stabled with MiMIC line from Herman Dierick) × w[*]; TI{2A-lexA::GAD}5-HT7[2A-lexA] (BDSC 84354)
- 2) **Fig. 3G and 4G:** UAS-RFP, Aop-GFP;5HT1B/Cyo (BDSC 3229 stabled with MiMIC line from Herman Dierick) × w[*]; TI{2A-lexA::GAD}5-HT7[2A-lexA] (BDSC 84354)
- 3) **Fig. 3H and 4H:** UAS-RFP, Aop-GFP;;5HT7/TM3 (BDSC 3229, stabled with MiMIC line from Herman Dierick) × w[*]; TI{2A-lexA::GAD}5-HT7[2A-lexA] (BDSC 84354).

Aim 1.2 Figures: Stochastic labeling of 5-HTR expressing vPN (Fig. 5, 6, and 7)

Fig. 1B, 5, 6, 7A:

w[1118] P{y[+t7.7] w[+mC]=hs-FLPG5.PEST}attP3; PBac{y[+mDint2]
w[+mC]=10xUAS(FRT.stop)myr::smGdP-HA}VK00005 P{y[+t7.7]
w[+mC]=10xUAS(FRT.stop)myr::smGdP-V5-THS-10xUAS(FRT.stop)myr::smGdP-FLAG}su(Hw)attP1
(BDSC 64085) × yw^{*};5HT1A 4464-T2A-G4/Cyo (gift from Dr. Herman Dierick)

Fig. 1C, 5, 6, 7B, 7C:

w[1118] P{y[+t7.7] w[+mC]=hs-FLPG5.PEST}attP3; PBac{y[+mDint2]
w[+mC]=10xUAS(FRT.stop)myr::smGdP-HA}VK00005 P{y[+t7.7]
w[+mC]=10xUAS(FRT.stop)myr::smGdP-V5-THS-10xUAS(FRT.stop)myr::smGdP-FLAG}su(Hw)attP1
(BDSC 64085) × yw^{*};5HT1B 5213-T2A-G4/Cyo (gift from Dr. Herman Dierick)

Fig. 5, 6, 7D:

w[1118] P{y[+t7.7] w[+mC]=hs-FLPG5.PEST}attP3; PBac{y[+mDint2]
w[+mC]=10xUAS(FRT.stop)myr::smGdP-HA}VK00005 P{y[+t7.7]
w[+mC]=10xUAS(FRT.stop)myr::smGdP-V5-THS-10xUAS(FRT.stop)myr::smGdP-FLAG}su(Hw)attP1
(BDSC 64085) × yw^{*};5HT2A 459-T2A-G4/TM6 (gift from Dr. Herman Dierick)

Fig. 5, 6:

w[1118] P{y[+t7.7] w[+mC]=hs-FLPG5.PEST}attP3; PBac{y[+mDint2]
w[+mC]=10xUAS(FRT.stop)myr::smGdP-HA}VK00005 P{y[+t7.7]
w[+mC]=10xUAS(FRT.stop)myr::smGdP-V5-THS-10xUAS(FRT.stop)myr::smGdP-FLAG}su(Hw)attP1
(BDSC 64085) × yw^{*};5HT2B 5208-T2A-G4/TM3 (gift from Dr. Herman Dierick)

Fig. 5, 6, 7E:

w[1118] P{y[+t7.7] w[+mC]=hs-FLPG5.PEST}attP3; PBac{y[+mDint2]
w[+mC]=10xUAS(FRT.stop)myr::smGdP-HA}VK00005 P{y[+t7.7]
w[+mC]=10xUAS(FRT.stop)myr::smGdP-V5-THS-10xUAS(FRT.stop)myr::smGdP-FLAG}su(Hw)attP1
(BDSC 64085) × UAS-RFP,Aop-GFP;;5HT7/TM3 (BDSC 32229, stabled with MiMIC line from Herman
Dierick)

Aim 1.3 Figures. 5-HTR expression of two i-vPN subpopulations (Fig. 8, 9, 10, an 11)

A) R86G06 subpopulation

w[1118]; P{y[+t7.7] w[+mC]=GMR86G06-lexA}attP40 (BDSC 54990) ×

- 1) **Fig. 8A, 8D, 9B, 11:** UAS-RFP, Aop-GFP;5HT1A/Cyo (BDSC 3229, stabled with MiMIC line from Herman Dierick, Gnerer et al. 2015), **AND**
- 2) **Fig. 9C, 11:** UAS-RFP, Aop-GFP;5HT1B/Cyo (BDSC 3229, stabled with MiMIC line from Herman Dierick), **AND**
- 3) **Fig. 9D, 11:** UAS-RFP, Aop-GFP;;5HT2A/TM3 (BDSC 3229, stabled with MiMIC line from Herman Dierick), **AND**
- 4) **Fig. 9E, 11:** UAS-RFP, Aop-GFP;;5HT2B/TM3 (BDSC 3229, stabled with MiMIC line from Herman Dierick), **AND**
- 5) **Fig. 9F, 11:** UAS-RFP, Aop-GFP;;5HT7/TM3 (BDSC 3229, stabled with MiMIC line from Herman Dierick).

B) R24H08 subpopulation

w[1118]; P{y[+t7.7] w[+mC]=GMR24H08-lexA}attP40 (BDSC 52732) ×

- 1) **Fig 10B, 11:** 10UAS-RFP, Aop-GFP;5HT1A/Cyo (BDSC 3229, stabled with MiMIC line from Herman Dierick), **AND**
- 2) **Fig 10C, 11:** UAS-RFP, Aop-GFP;5HT1B/Cyo (BDSC 3229, stabled with MiMIC line from Herman Dierick), **AND**
- 3) **Fig 10D, 11:** UAS-RFP, Aop-GFP;;5HT2A/TM3 (BDSC 3229, stabled with MiMIC line from Herman Dierick), **AND**
- 4) **Fig 10E, 11:** UAS-RFP, Aop-GFP;;5HT2B/TM3 (BDSC 3229, stabled with MiMIC line from Herman Dierick), **AND**
- 5) **Fig 8B, 8E, 10F, 11:** UAS-RFP, Aop-GFP;;5HT7/TM3 (BDSC 3229, stabled with MiMIC line from Herman Dierick).

C) R24H08 and R86G06 combination

Figure 8H, 8I: w[1118]; Aop-RFP, UAS-GFP;GMR86G06Gal4 (BDSC 67093 stabled with BDSC 93199) ×

w[1118]; P{y[+t7.7] w[+mC]=GMR24H08-lexA}attP40 (BDSC 52732)

Table 1. Genotypes used in Chapter 2 Aim 2.

Figure No.	Genotype	Source
Fig. 12	w[11118]; P{y[+t7.7] w[+mC]=GMR86G06-GAL4}attP2	BDSC 40468
Fig. 12	w[11118]; R24H08-p65.AD; VT046303-Gal4.DBD	BDSC 69049 and BDSC 74612
Fig. 12	y[1] v[1]; P{y[+t7.7] v[+t1.8]=TRiP.JF02576}attP2	BDSC 27273
Fig. 12	y[1] v[1]; P{y[+t7.7] v[+t1.8]=TRiP.JF01852}attP2	BDSC 25834
Fig. 12	y[1] v[1]; P{y[+t7.7] v[+t1.8]=UAS-GFP.VALIUM10}attP2	BDSC 35786
Fig. 12	y[1] v[1]; P{y[+t7.7]=CaryP}attP2	BDSC 36303
Fig. 12	w[11118]	BDSC 6326

Table 2. Antibodies used for immunocytochemistry.

Antigen	Species, Manufacturer, Catalog #	Dilution Ratio	Incubation Time (hr)
GFP	Chicken (Abcam, #ab13970, RRID: AB_300798)	1:500	24
RFP	Rabbit (Rockland, #600-401-379, RRID: AB_828390)	1:500	24
HA-Tag	Rabbit (CST, #3724, RRID: AB_10693385)	1:300	48
N-Cadherin	Rat (DSHB, #DN-Ex, RRID: AB_528121)	1:250	48
AlexaFluor-488 (Chicken)	Donkey (Jackson ImmunoResearch Laboratories, #703-545-155, RRID: AB_2340375)	1:1000	24
AlexaFluor-488 (Rabbit)	Goat (Molecular Probes, #A-11008, RRID: AB_143165)	1:1000	24
V5: Dylight-550	Mouse (Bio-Rad, #MCA1360D550GA, RRID: AB_2687576)	1:500	24
AlexaFluor-546 (Rabbit)	Donkey (Invitrogen, #A-10040, RRID: AB_2534016)	1:1000	24
AlexaFluor-647 (Rat)	Donkey (Abcam, #ab150155, RRID: AB_2813835)	1:1000	24

Table 3. Predicted Odor Valence of Analyzed Glomeruli.

Odor Class	OSN receptor	Odors	Odor Valence	Reference
D	Or69a	ethyl 3-hydroxyhexanoate, alpha-terpineol, linalool		Knaden et al. 2012
DA1	Or67d	11-cis-vaccenyl acetate (cVA)		Kurtovic et al. 2007
DA2	Or56a	Geosmin		Stensmyr et al. 2012
DA3	Or23a	1-pentanol, 2-hexanol, 1-hexanol		Knaden et al. 2012
DA4	Or43a and Or2a	1-hexanol, cyclohexanol, cyclohexanone, 3-hydroxy-2-butanone, isopentyl acetate		Knaden et al. 2012
DC1	Or19a	valencene, (-)-caryophyllene oxide		Knaden et al. 2012
DC2	Or13a	1-octen-3-ol, 2-heptanol		Knaden et al. 2012
DC3	Or83c	Farnesol, 3-hexanol, 2-methylcyclohexanol		Ronderos et al. 2014; Jeanne et al. 2018
DC4	Or64a	acetic acid, phenylacetic acid, butyric acid, 2-oxovaleric acid, propanoic acid, water		Knaden et al. 2012
DL1	Or10a	methyl salicylate, Ethyl benzoate, acetophenone, methyl benzoate		Knaden et al. 2012
DL2d	Or75abc	-3 butyric acid		Getahun et al. 2012
DL2v	Or75abc	-3 butyric acid		Getahun et al. 2012
DL3	Or65a	pyrrolidine, 6-methyl-5-hepten-2-one		Silbering et al. 2011; Min et al. 2013

DL4	Or49a	2-heptanone, 1- hexanol		Knaden et al. 2012
DL5	Or7a	E2-hexenal, E2-hexenyl acetate, benzaldehyde		Knaden et al. 2012
DM1	Or42b	3-hexanone, ethyl (S)-(+)-3-hydroxybutanoate, 3-penten-2-one, ethyl propionate, 2-hexanol		Knaden et al. 2012
DM2	Or22a	Ethyl hexanoate, methyl hexanoate		Knaden et al. 2012
DM3	Or47a	pentyl acetate, butyl acetate, methyl hexanoate, propyl acetate		Knaden et al. 2012
DM4	Or59b	methyl acetate, ethyl acetate, methyl 2-methylpropanoate		Knaden et al. 2012
DM5	Or85a	ethyl 3-hydroxybutyrate, E3-hexanol, 1-hexanol		Knaden et al. 2012
DM6	Or67a	butyl propanoate		National Center for Biotechnology Information (2022)
DP1l	Ir75a	acetic acid, 2,3-butadione, propionic acid		Knaden et al. 2012
DP1m	Ir64a	2,3-butanediol, 2,3-butanedione, 2-oxovaleric acid, acetic acid		Knaden et al. 2012
V	Gr21a	Carbon Dioxide		Turner and Ray 2009
VA1d	Or88a	pyrrolidine, methyl palmitate, methyl laurate, methyl myristate		Silbering et al. 2011; Min et al. 2013; Jeanne et al. 2018
VA1v	Or47b	(S)-(+)-carvone, palmitoleic acid		Lone et al. 2015; Jeanne et al. 2018
VA2	Or92a	2,3-butanedione, 2,3-butanediol, ethyl (S)-(+)-3-hydroxybutanoate		Knaden et al. 2012

VA3	Or67b	acetophenone, Z3-hexanol, phenethyl alcohol, 1-hexanol		Knaden et al. 2012
VA4	Or85d	ethyl pentanoate, 2-heptanone, 6-methyl-5-hepten-2-one		Knaden et al. 2012
VA5	Or49b	2-methylphenol, 3-methylphenol, 4-methylphenol		Knaden et al. 2012
VA6	Or82a	geranyl acetate		Knaden et al. 2012; Jeanne et al. 2018
VA7I	Or46a	4-methylphenol		Knaden et al. 2012
VA7m	Orphan, IR41a/IR7 6b (VC5)	(Putrescine, spermidine, pyridine, cadaverine)		Knaden et al. 2012
VC1	Or33c	cyclohexanone, 2-heptanone, fenchone		Knaden et al. 2012
VC2	Or71a	eugenol, 2-methylphenol, 4-methylphenol, methyl salicylate		Knaden et al. 2012
VC3I	Or35a	1-heptanol, 1-hexanol, E2-hexenyl acetate, hexyl butyrate, E2-hexenol, 3-methyl-butanol, 1-octanol		Knaden et al. 2012
VC3m	Or35a	alcohols and ketones		Knaden et al. 2012
VL1	Ir75d	pyrrolidine		Silbering et al. 2011; Min et al. 2013
VL2a	Ir84a	phenylacetaldehyde, phenylacetic acid		Knaden et al. 2012
VL2p	Ir31a	2-oxovaleric acid, 2-oxopentanoic acid		Prieto-Godino et al. 2017
VM1	Ir92a	dimethylamine		Min et al. 2013

VM2	Or43b	ethyl trans-2butenoate, ethyl butyrate, isobutyl acetate, methyl butyrate, propyl acetate, 2,2-hexanol, ethyl propionate, 2-pentanol		Knaden et al. 2012
VM3	Or9a	3-hydroxy-2-butanone, 2,3-butanediol, 2-pentanol, diethyl phosphate		Knaden et al. 2012
VM4	Ir76a	acetic acid		Knaden et al. 2012
VM5	Or85b and OR98a	butyl acetate, E3-hexenol, methyl hexanoate, 3-octanol, 2-heptanone		Knaden et al. 2012
VM6	Ir40a	N/A (Hydrosensation with VP1)		Knecht et al. 2017
VM7	Or59c(v), Or42a (d)	ethyl butyrate, 6-methyl-5-hepten-2-one, 3-octanol, propyl acetate, 2-butanoate, ethyl acetate, 2,3-butanedione		Knaden et al. 2012

Crossing Schemes: Aim 1.1. For 5-HTR-T2A-G4 and 5-HTR-LexA co-expression, only vPN cell bodies that have a visible connection to the AL fascicle were assessed. Co-expression is assessed by overlapping the GFP and RFP channels. Both i-VPNs and e-VPN populations were analyzed. Out of the five total 5-HTR-LexA lines, two lines, 5-HT1A-LexA and 5-HT1B-LexA were not included because some 5-HTR population cell clusters did not match the verification that was already made with the 5-HTR-T2A-Gal4 line. The 5-HT2A-LexA was excluded for both e-VPNs and i-VPNs as the 5-HT2A-LexA e-PN were not visible which is not consistent with the 5-HT2A-MiMIC Gal4 line. I did not include data from the 5-HT2AR-LexA as the 5-HT2AR-Gal4 has expression in i-VPNs but do not show expression in e-VPNs. We did observe e-VPN innervations in the 5-HT2AR-T2A-Gal4 which makes the 5-HT2AR lines questionable for 5-HTR co-expression analysis. We also ran issues with getting duplicates since the line lost its 5-HTAR expression during the pandemic both in the lab and the fly stock supplier. We decided to remove the data due to the line being problematic. Further, I did not have sufficient time to compare the 5-HT2B and 7 LexA expressions with the 5-HT2A-MiMIC Gal4 line expression.

Differences in vPN expression between the 5-HTR-LexA and 5HTR-T2A-G4-MiMIC lines likely arise from the method used to construct these lines. Preference is given to the 5-HTR-T2A-G4-MiMIC as predictions made using these lines in the visual system were verified using single-cell RNAseq (Sampson et al. 2020). RNAseq of OSNs verified that the 5-HT2BR are expressed by OSNs (Bryson et al. 2021), consistent with predictions made using the 5-HT2B-T2A-MiMIC-Gal4 (Sizemore and Dacks 2016).

Aim 1.2. Each given 5-HTR-T2A-Gal4 MiMIC line male was crossed separately with the MCFO line virgins (BDSC #64085). After 48 hours, the progeny was subjected to heat shock at 37°C between 0 to 10 minutes depending on the quality of vPN expression in the final product from previous scans. The optimized heat-shock period for given 5-HTR is as the following; 0-2 minutes for 5-HT1A, 5-HT1B, and 5-HT2A, 0-10 minutes for 5-HT2B, and 10 mins with 5-HT7. Next, additional preparations step were done for 5-HT2B and 5-HT7 crosses. This is due to the presence of OSNs (expressed by 5-HT2B), or the Johnston's Organ Neurons (JONs, expressed by 5-HT7) occluding the view of glomerular innervation by the vPNs within the AL and vPN cell bodies near the AMMC, respectively. Antennae of 1-to-2-day old 5-HT2B and 5-HT7 flies were ablated and the animals were heat-shocked after 48 hours. All MCFO brain dissections were done between 2 to 10 days post heat shock.

The total number of AL scanned for each 5-HTR-T2A-Gal4 was determined based on the Coupon Collector's problem (reviewed in Lobo et al. 2020), which predicts the number of random draws needed to obtain each coupon type in a container. We determined the number of AL scans needed based on published cell body counts of vPNs of each 5-HTR-T2A-Gal4 (Sizemore and Dacks 2016). The numbers for AL scans for each 5-HTR are determined as the following; 50 (n=25 brains) for 5-HT1A, 50 (n=25 brains) for 5-HT1B, 15 (n=7.5 brains) for 5-HT2A, 46 (n=23 brains) for 5-HT2B, and 55 (n=27.5 brains) for 5-HT7.

Determination of Glomeruli Odor Valence (Refer to Table 3). Each glomeruli were identified using previously established diagrams of the AL (Laissue et al. 1999; Couto et al. 2005; Task et al. 2022). For every 47 glomeruli, its OSN expression is obtained through an established dataset (Grabe et al. 2016). Each olfactory receptor associated with a glomerulus is typed into the DoOR database (Münch and Galizia 2016, <http://neuro.uni-konstanz.de/DoOR/default.html>) and the odorant that evoke the strongest responses was selected. The odor valence was determined from previously behavioral assays using the odor (Kurtovic et al. 2007; Turner and Ray 2009; Silbering et al. 2011; Getahun et al. 2012; Knaden et al. 2012; Stensmyr et al. 2012; Min et al. 2013; Ronderos et al. 2014; Lone et al. 2015; Knecht et al. 2017; Prieto-Godino et al. 2017; Jeanne et al. 2018, National Center for Biotechnology Information 2022). A glomerulus is defined as attractive if the odorants that evoke the strongest response consist of either attractive or both attractive and neutral odors. OSNs were classified as evoking aversion if the odorant evoking the strongest response is either aversive or a combination of both aversive and neutral odors. A glomerulus that expressed both odor valence is defined as both. According to Table 3, glomeruli are color-coded according to encoding attraction (Dark Green), aversion (Light red), neutral (Light Orange), and Multiple valences (attraction and aversion, Light blue).

vPN analysis: Aim 1.2. A few criteria were used for single clones to be included in the matrix depicted in Figure 5. First, the vPN should enter the AL via the AL fascicle and project to the higher brain regions via the mALT and mlALT as described in previous papers (Sizemore and Dacks 2016). Secondly, the vPN cell bodies and glomerular innervation patterns had to be visible and distinguishable from other cell bodies entering the AL. Lastly, only glomerular innervations connected to the primary neurites that originate from the AL fascicle as well as an exit out the mlALT or mALT were counted as positive innervations (Figure 1).

Aim 1.3. Using the Flylight database (<https://flweb.janelia.org/cgi-bin/flew.cgi>, Jenett et al. 2012), we selected driver lines that have intensity values of expression between 3-5, and distribution values between 1-3 in the search settings. For vPN-LexA and 5-HTR-T2A-Gal4 crosses, glomerular innervations were analyzed similarly to Aim 1.1 and vPN-5-HTR co-expression was done similarly to Aim 1.2. Glomerular innervation data were tabulated into a matrix.

Immunocytochemistry: Brains were dissected in *Drosophila* External Saline (CSHL recipe 2011; used in Sizemore and Dacks 2016) and fixed in 4% paraformaldehyde containing 0.02% TX (Triton-X) for 30 – 60 minutes on ice (Protocol described in Sweeney et al. 2011). The samples were then washed repetitively (4x, once every 15 minutes) with PBST (Phosphate Buffer Saline in 0.5% TX) and later blocked for 60 minutes in PBST containing 4% BSA (Bovine Serum Albumin). Next, samples were incubated for 48 hours at 4°C with primary antibodies in PBST containing 5mM Sodium Azide. Similar washing and blocking were repeated similar on Day 3 and incubated with secondary antibodies. On Day 5, brains were washed twice with PBST and twice with PBS, then run through an ascending glycerol series (40%, 60%, and 80% glycerol in water respectively). Brains were mounted in VectaShield (Vector

Labs Burlingame, CA #H-1000) on good slides and scanned using the Olympus confocal microscope FV1000 equipped with a 40x silicon oil immersion lens. Images were viewed and analyzed using Olympus FluoView software and processed using Inkscape and CoreIDRAW vector quality graphics software.

Behavioral Assay Fly Stocks: Flies were raised on Nutri-Fly® MF, Molasses Formulation (Genessee, Cat. #66-123) at 50% humidity and 25°C on a 12:12 dark-light cycle. In total, five lines were used; R86G06-Gal4, UAS-5-HT7R-RNAi, and three control lines (W1118, attP2, and UAS-GFPVALIUM10).

T-maze assay: The T-mazes were created by attaching two caps of two bacteria culture tubes (12x75mm Polystyrene Tubes with Dual Positions Polyethylene Caps, USA Scientific, Cat. #8576) inserted onto a T-junction (Industrial Specialities manufacturing, TA-14-PP 1/4" Hose Barb T-junction, Natural Polypropylene). Each cap was hollowed out using a hot knife and secured at each horizontal end of the T-junction. Next, a funnel was created using a fine pipette tip (Samco Scientific, Cat. #232-11) to connect the vertical end of the T-junction to the START test tube vial. ODOR vials were labeled with red tape while CONTROL vials were labeled in green and attached to the horizontal end. 1-often-3-ol (Sigma-Aldrich, Cat. #3391-86-4) was used as the odorant. These odors were serially diluted with mineral oil (Sigma-Aldrich, Cat. #).

After 10 days, virgin and male flies were collected from each parental stock bottle within seven days. Within days 5-7, the following crosses were made:

- vPN-Gal4 Males > UAS-GFP-Valium10 virgin females
- vPN-Gal4 Males > UAS-5HTR-RNAi virgin females
- W1118 Males > attP2 virgin females
- W1118 Males > UASGFP-Valium10 virgin females
- attP2 Males > vPN-Gal4 virgin females
- UAS-5HTR-RNAi Males > W1118 virgin females

For each bottle, 15-30 virgin females were crossed with 7 males of the other genotype. Two sets of each bottle were made to maximize progeny yield. After 5 days, the parents from previous crosses were pushed into new bottles and supplemented with new female virgins. The recently pushed parents were removed after 5 days. The F1 progeny were collected after 10 days. During the collection, 25 females and 1 male were separated into small food vials (Genessee, Drosophila Vials, Narrow (PS) Polystyrene, Cat. #32-116SB) up to a total of 8 vials per genotype. This collection process was done every other day. Each food bottle was discarded after day 10.

Four days after eclosion, flies were starved for 18-20 hours in vials containing KimWipes moistened with 1mL of diH2O. The experiment was double-blinded to remove bias when loading the animals and counting the final results. The following day, the behavioral assay was conducted. The

filtered paper was cut into 5x3 mm pieces and inserted into separate plastic test tube vials labeled ODOR and CONTROL. 30 microliters of tested odor and its control solvent were pipetted into each respective horizontal arm using filtered multi-barrier tips.

T-mazes assembly was done under red-light conditions to avoid the influence of light on fly behavior. First, the starved flies were anesthetized under ice and loaded into the start vial through a funnel. Each T-maze was secured on a test tube rack with the CONTROL and ODOR arms alternating inside and outside the test tube rack. The T-junction was adjusted to ensure that the horizontal arms are perpendicular to the start vials. The test tube rack containing the vials was loaded into the incubator for 24 hours at 32°C and 70-80% RH. After 24 hours, the test tube racks were placed in a freezer for 90 minutes. The results were collected by counting flies that are present within each arm. Then, the performance and participation index of the flies were calculated. The performance index determines the average fly's perception of a given odor (Attraction or Aversion). The performance index determines the number of flies that participated in the trial run. Both formulas were calculated below:

Performance Index:

$$\frac{(\#Flies \text{ in Odor Arm} - \#Flies \text{ in Control Arm})}{\text{Total \#Flies}}$$

Participation Index:

$$\frac{(\#Flies \text{ in Odor Arm} + \#Flies \text{ in Control Arm})}{\text{Total \#Flies}}$$

All data were entered into Microsoft® Excel and statistical analysis was done using GraphPad Prism 5 (GraphPad Software Inc.). Performance Index of flies with a Participation Index of a value of 0.30 or greater was selected. An n value of 15 was used for each cross. For the statistical analysis, the samples were run through D'Agostino normality test to determine the next suitable analysis. If the sample passed the normality test, one ANOVA was done to determine the p-value. If samples do not pass the normality test, a Kruskal-Wallis's test was done to determine the significance of the dataset.

Equipment Cleaning: The starving vials and T-maze components were emptied and sorted into respective groups. First, 15g of Alconox was measured and dissolved in separate buckets containing 2L of water. The following components were loaded into each bucket and vigorously mixed until each part is coated with soapy water. After soaking overnight, a test tube brush was used to scrub each T-maze component. Each component was washed thoroughly (approximately 3 times) using a strainer under hot water. Then, the components were sprayed with 70% ethanol and left to air dry for 15 minutes. Finally, the components were rinsed with distilled tap water before being loaded into a 50°C-dryer oven overnight. Similar processes were done with the starving vials except that it was air-dried on a clean lab mat overnight.

Fly Arena Assay: 1% Agar solution was made using 100mg of Bactero-Agar (Benton, Dickinson, and Co., REF# 214010) and 10mL of diH₂O in a flask. The mixture was heated and dissolved using a microwave until a clear solution was formed. Under a fume hood, 25ul of agar solution was pipetted onto on edge of a petri dish (35mm x 10mm Petri Dish, Sterile, CELLTREAT Scientific Products, Cat#229638 and Falcon 35mm Bacteriological Petri Dish, CORNING, Cat#351008). Next, the odor of interest is pipetted into the flask to match the tested concentration ratio. 25ul of that odor-agar solution was later pipetted on the opposite side of the petri dish. The agar is left to set and the equipment used was thoroughly cleaned and wiped with distilled water and ethanol. The experiment was carried out using an OptoBox containing a Flea3.1 USB3 Camera (Point Grey (discontinued), FL3-U3-13Y3M-C) equipped with an IR lens (Thorlabs, MVL6WA) and an Arduino Uno Rev 3 microcontroller (Arduino, A000066). The recordings were done using Point Grey FlyCap2 version 2.11.3.121 and MATLAB 2018, which records 900 seconds in two separate intervals at 60FPS. Before running the script, 18-20 hour starved female flies (same procedure as the T-maze arena) were cold anesthetized for 2 minutes. The agar-containing petri dish was placed onto the IR light stage. Three female flies were placed at the center in between the two agar droplets. A petri dish lid was used to cover the topside and a Matlab script was run. After the completion of a recording, the previous flies were removed and replaced with a new set of flies of the next genotype. The video files from each genotype were collected. An n value of 20 was used for each cross.

Three main pieces of information were collected from each video file; 1) XY position of each fly for a total of 108,000 frames, 2) XY coordinates of each agar droplet, and 3) the diameter of the petri dish arena. The first information was obtained using the FlyTracker Matlab script from Perona Lab (reviewed in Leng et al. 2020) while the last two data using Fiji image processing software. All the data points were compiled into Microsoft® Excel. The first 18000 frames (5 minutes) were removed to account for fly recovery after cold anesthesia. The XY distance between each fly and agar source was calculated and averaged. The performance index is obtained by determining the average x and y distance of the flies with an agar source within the total 90,000 frames calculated. The approximate area of control by each agar was determined using the Goat Problem (Hoffman 1998). Within the arena, there will be three zones; 1) An odor-occupied zone, 2) a control-occupied zone, and 3) a neutral zone. Based on that distance, we determine whether the response is an attraction or aversion. This value is then compiled into GraphPad Prism 5 (GraphPad Software Inc.) where statistical analysis (similar to the T-maze assay) was done.

Results:

vPNs express a combinatorial 5-HTR co-expression pattern.

If we assume that vPNs do not co-express 5-HT receptors, the individual counts for vPNs that express 5-HTRs provide an estimate of ~60 vPNs (Sizemore and Dacks 2016), almost half of the currently known ~144 vPNs (Bates et al. 2020). Knowing that all 5-HTRs are expressed by the vPNs populations (Sizemore and Dacks 2016), we hypothesize that vPNs could have three 5-HTR expression patterns; 1) No co-expression among vPNs (“no overlap”), 2) All 5-HTRs are expressed by each vPN (“complete overlap”), or 3) A diverse set of 5-HTR co-expression patterns exist (“combinatorial”) (Figure 2).

To determine if a vPN can express multiple 5-HTRs, we compared the expression of LexA driver lines for each 5-HT receptor type (Deng et al. 2019) with the expression of the established 5-HTR-T2A-MiMIC lines used previously (Gnerer et al. 2015; Sizemore and Dacks 2016). Out of the five receptors, the 5-HT1AR-LexA, 5-HT1BR-LexA, and 5-HT2AR-LexA were not included as either their expression in vPNs cell bodies did not match the 5-HTR-T2A-Gal4-MiMIC lines (Gnerer et al. 2015) or they were missing keystone cell clusters of a neuron known to express a given 5-HTR (for instance, the 5-HT1AR-LexA do not express in MIPergic LNs neurons that innervate the AL and are known to express the 5-HT1AR (Tyler Sizemore, unpublished results)).

We examined both the i-vPNs and e-vPNs of each AL scan (Figures 3 and 4). To be consistent, we use the total cell body count expressed by the LexA line to determine the percent co-expression between two receptor types. The 5-HT2BR-LexA line has the most successful expression rate (i.e., easily distinguishable cell body clusters, consistent cell body counts, least error in immunocytochemistry preparation) for both i-vPN and e-vPN populations than the 5-HT7R-LexA counterpart. We found that 5-HT2B-LexA lines are likely to co-express with 5-HT7R (40%), then 5-HT1AR (30%), and finally 5-HT1BR (13%) (Figure 3). While e-vPNs were likely to co-express the 5-HT2B and the 5-HT7 (43%), they were more likely to co-express with the 5-HT1BR (24%) than the 5-HT1AR (17%).

Within 5-HT7R-LexA i-vPNs, co-expression is mostly seen with 5-HT1AR (31%) followed by 5-HT1BR (15%) (Figure 3). We did not test 5-HT7R-LexA with the 5-HT2B-T2A-Gal4 as the 5-HT7-T2A-Gal4 was already tested with the 5-HT2BR-LexA. 5-HT7R e-vPNs share an opposite pattern, having more co-expression with 5-HT1BR (36%) followed by 5-HT1AR (25%) (Figure 4).

Taken altogether the degree of co-expression different each LexA-Gal4 combination differs for both i-vPN and e-vPN populations. For example, i-vPNs have a higher preference for 5-HT1AR co-expression compared to 5-HT1BR by half (Figure 3). e-vPNs has a similar co-expression preference for both. Further, 5-HT7R co-expression patterns for the 5-HT2B-LexA line are consistent for both i-vPN and

e-vPN populations. Taken together, this analysis confirms a degree of combinatorial 5-HTR co-expression exists within this population of vPNs.

Stochastic expression of a total 5-HTR population reveals diverse vPN innervation patterns within each population.

The next goal was to determine if a vPN expressing a given 5-HTR would innervate different AL glomeruli and LH regions. That would suggest that 5-HT modulation behaves in a stimulus-specific manner. We conducted a Multi-Color Flip-Out (MCFO) screen of each 5-HTR-T2A-Gal4 line to locate vPNs from both the i-vPN and e-vPN clusters. MCFO is a technique that conditionally expresses multiple smGFPs bound to epitope markers upon heat shock activation (Nern et al. 2015). This allows us to stochastically observe the innervation patterns of vPNs in the AL and the LH based on the 5-HTRs expressed.

vPN expression throughout all the 5-HTR-T2A-Gal4 varies, with some requiring a longer heat shock to observe our vPNs of interest. My scans contained either one of three combinations; only e-vPN, only i-vPN, or a mixture of both. In some cases, we could not distinguish the processes of individual vPNs within a mixture combination, therefore we represent the 5-HTR expression matrix as a contribution of both vPN subtypes to a single AL (Figure 5). This study only constitutes vPNs that were most likely to be expressed using MCFO and therefore not a comprehensive survey to study all vPNs that express a given 5-HTR. We did this analysis across 47 glomeruli, merging some glomerulus to become one (DA4l and DA4m, VM5d and VM5v, VA1l and VA1m).

For the 5-HT1AR, 5-HT1BR, 5-HT2AR, and 5-HT2BR, MCFO resulted in the e-vPNs being more likely to be expressed than i-vPNs. Cell bodies within each scan vary from 1 to 20 cells, depending on the effect of the heat shock treatment. The percent of samples with only in e-vPNs for the 5-HT1AR was 70%, 5-HT1BR was 94%, 5-HT2BR was 96% and the 5-HT2AR was only observed expressed in e-vPNs. On the other hand, 5-HT7R has the most scans containing only i-vPNs (5-HT7R = 96%). Further, MCFO using the 5-HT1AR-T2A-MiMIC lines generated samples with the highest proportion of a combination of both e-vPN and i-vPNs in an AL (5-HT1AR = 28%) (Example in Figure 7A).

Based on the different population glomerular innervation patterns (Figure 5), We noticed similar glomerular innervation trends when we compared the 5-HT1AR with 5-HT1BR expressing vPNs and the 5-HT2A with 5-HT2B expressing vPNs. In addition, the total of all 5-HT7R expressing vPNs innervates mostly glomeruli in the AL (42 out of 47 glomeruli). Then, I constructed a glomerular heat map based on the percent innervation by vPNs that innervate a given glomerulus for each 5-HTR (Figure 6). This approach would enable us to understand what combinations of vPNs that express each 5-HTR innervate a given glomerulus. I analyzed the innervation patterns of each receptor type based on 1) the valence of these glomeruli, 2) the combinatorial patterns that could exist within a glomerulus, and 3) the coarse plane within the AL (anterior, posterior, dorsal, ventral, medial, lateral) innervated by a given 5-HTR

expressing vPN. I also analyzed the data across three different levels, 1) glomeruli that are innervated by 50% of a 5-HTR expressing vPN population, 2) the top 15 glomeruli expression for each 5-HTR type, and 3) glomeruli that have 0 percent innervation.

Twelve glomeruli were innervated in more than 50% of samples, four glomeruli are shared among two 5-HTR, two glomeruli shared among three 5-HTR, and one glomerulus by four 5-HTR expressing vPNs populations. Of these, seven glomeruli respond to attractive odors (DC3, DM4, VA1d, VA1v, VA6, VA7m, and VL1), four respond to aversive odors (DL1, VA3, VA5, VA7l), and one glomerulus responding to both attractive and aversive odors (VC2) (Refer Table 3). Among these different glomeruli, 5-HT1AR expressing vPNs responds to 6 of 12 glomeruli, four of them encoding attractive odorant (VL1, VA1d, VA7m, and DC3) and two encoding aversive odorants (VA7l and VA5). Next, vPNs expressing 5-HT1BR respond to 7 of 12 glomeruli, five are attractive (VA1d, VA6, VL1, DC3, and VA1v) and two are aversive (VA5 and VA3) encoding glomeruli. Further, 5-HT2AR expressing vPNs respond to 2 of 12 glomeruli, one attractive (VA1d) and one aversive (DL1) while 5-HT2BR expressing vPNs responds to 7 of 12 glomeruli, of them three are attractive (VA7m, DC3, and VA1d) and three are aversive (VA7l, DC3, VA1d), and one responding to both valences (VC2). Lastly, 5-HT7R expressing vPNs respond to 1 of 12 glomeruli, to the attractive encoding DM4 glomeruli.

Some of the 12 glomeruli were innervated by a combination of vPNs expressing a given 5-HTR. For instance, VA1d is innervated by four 5-HTRs vPNs (1A, 1B, 2A, 2B) while DC3 and VA5 by three 5-HTR expressing vPNs (1A, 1B, and 2B). In addition, multiple combinations of two 5-HTR expressing vPNs were observed in glomeruli such as VA7m (1A, 2B), VA7l (1A, 2B), VA3 (1B, 2B), and VL1 (1A, 1B). The single glomerulus exclusively innervated by a 5-HTR expressing vPN is DL1 (1B), VA1v (1B), VA6 (1B), DM4 (7), and VC2 (2B). In terms of planes where the glomeruli are innervated, vPNs expressing the 5-HT1AR, 5-1B, 2A, and 2B innervated glomeruli located within the anterior, ventral, and lateral regions of the AL while vPNs expressing 5-HT7R innervated the posterior, dorsal, and medial regions of the AL.

I found a different combinatorial pattern of 5-HTR expression when I analyzed the top 15 glomeruli innervated by vPNs expressing 5-HTRs. Within this analysis, our 5-HTR expressing vPNs innervate 28 different glomeruli, 9 glomeruli innervated only by vPNs that express a single 5-HTR and 19 glomeruli innervated by vPNs expressing combinations of 5-HTRs. Out of these 28 glomeruli, 15 respond to attractive odors (DC3, DL2d, DL2v, DM1, DM4, DM6, DP1m, DP1l, VA1d, VA1v, VA2, VA6, VA7m, VL1, and VM5), nine respond to aversive odors (D, DA1, DC2, DL1, DL5, VA3, VA5, VA7l, and VC3m), one responding to both attractive and aversive (VC2) and three responding to neutral odors (DC1, VA4, and VC1) (Refer Table 3).

Based on the top 15 innervated glomeruli for each 5-HTR expressing vPNs, results show that 5-HT1AR, 1B, 2A, and 2B expressing vPNs almost equally innervate glomeruli encoding attractive and aversive odors while 5-HT7R expressing vPN has a stronger preference for glomeruli encoding attractive odors. The glomeruli valence for each 5-HTR expressing population is that 5-HT1AR expressing vPNs

encode eight attractive (VL1, VA1d, VA7m, DC3, VA1v, VA6, VM5, and VA2), five aversive (VA7I, VA5, DL1, VA3, and VC3m), and one neutral (VC1) glomeruli while 5-HT1BR expressing vPNs encode 6 attractive (VA1d, VA6, VL1, DC3, VA1v, and VA7m), seven aversive (VA5, VA3, DC2, VA7I, D, DL5, and DL1), and one neutral (DC1) glomeruli. Further, 5-HT2AR expressing vPNs encode seven attractive (VA1d, VA7m, VA6, DC3, DM6, DL2v, and VA2), five aversive (DL1, DL5, VA7I, VA5, and DC2), and two neutral (DC1 and VA4) glomeruli while 5-HT2BR expressing vPNs encode seven attractive (VA7m, DC3, VA1d, VA2, VA1v, and DL2d), six aversive (VA1I, VA3, VA5, DC2, DA1, DL5, and DL1), and one neutral (DC1) glomeruli. Then, 5-HT7R expressing vPNs respond to ten attractive (DM4, DL2d, DL2v, VL1, VM5, DP1I, DP1m, VA7m, and DC3), two aversive (DC2 and VA7I), and three neutral (DM1, DC1, and VC1) glomeruli. Under this comparison, all 5-HTR expressing vPNs to a degree innervate the VC2 glomerulus which encodes multiple odor valences. The 19 glomeruli that were innervated by vPNs by more than one 5-HTR-T2A-MiMIC line show a broad range of 5-HTR type combinations. First, four glomeruli (DC3, VA7m, VA7I, and VC2) were innervated by vPNs from all five 5-HTR-T2A-MiMIC lines populations. Next, five glomeruli are innervated by four 5-HTR expressing vPNs types, of them, three glomeruli were innervated by all except the 5-HT7R expressing vPNs (VA1d, DL1, and VA5), while two are innervated by all except 5-HT1AR vPNs (DC1, DC2). Further, six groups of glomeruli were innervated by vPNs expressing three different 5-HTRs expressing vPNs. For example, VA1v and VA3 are innervated by 5-HT1AR, 1B, and 2B expressing vPNs, VA6 is innervated by 1A, 1B, and 2A expressing vPNs, VA2 is innervated by 1A, 2A, and 2B expressing vPNs, DL5 is innervated by 1B, 2A, and 2B expressing vPNs, and VL1 is innervated by 1A, 1B, and 7 expressing vPNs. There are four glomeruli innervated by only two populations of 5-HTR expressing vPNs. VC1 and VM5 are by 1A and 7 expressing vPNs, DL2v is innervated by 2A and 7 expressing vPNs, and DL2d is innervated by 2B and 7 expressing vPNs. Moreover, a total of nine glomeruli expressing vPNs are innervated by only one 5-HTR expressing vPN. 5-HT7R expressing vPNs innervated four glomeruli (DM1, DM4, DP1m, and DP1I), 2A expressing vPNs innervated two glomeruli (DM6 and VA4), and one glomerulus was innervated by vPNs that express 1A (VC3m), 1B (D), and 2B (DA1) expressing vPNs.

Finally, 14 glomeruli had no innervations from two or more 5-HTR types and 8 glomeruli had no innervation from only one 5-HTR type. Of these total 22 glomeruli, 14 respond to attractive odors (DA3, DC4, DL2d, DL3, DM4, DP1I, DP1m, VA1v, VL1, VL2a, VL2p, VM1, VM4, and VM5), 3 respond to aversive odors (V, VC3I, and VC3m) and 5 respond to neutral odors (DL4, DM1, DM2, VC1, and VM6). Among the 22 glomeruli that received no innervations from 5-HTR expressing vPNs, 5-HT2AR expressing vPNs likely did not innervate the greatest number of glomeruli (18 of 22), of them 11 are attractive (VM1, DA3, DP1m, DL2d, DM4, DP1I, VA1v, VL1, VL2a, VM5, and VM4), three aversive (VC3I, VC3m, and V) and four neutral (DL4, DM1, VC1, VM6) encoding glomeruli. Next, 5-HT1BR expressing vPNs likely did not innervate eight glomeruli, five are attractive (DC4, DP1I, DP1m, and VL2p), one aversive (V), and two neutral (DL4 and DM1) encoding glomeruli. Both 5-HT1AR and 1BR expressing vPNs likely did not innervate six glomeruli. For 5-HT1AR expressing vPNs, three are attractive (DC4, VM1, and DM4), one

aversive (V), and two neutral (DM1 and VM6) encoding glomeruli while 5-HT2BR expressing vPNs likely did not innervate two attractive (VM1 and VL2p), two aversive (VC3l and VC3m) and two neutral (DL4 and DM2) encoding glomeruli. Lastly, 5-HT7R expressing vPNs likely did not innervate only five glomeruli, three are attractive (DA3, DL3, and VL2a), one aversive (V), and one neutral (DL4) encoding glomeruli.

A few specific glomeruli were unlikely to be innervated by multiple 5-HTR expressing vPNs. Glomeruli DL4 was not innervated by all except 5-HT1AR expressing vPNs, VM1 by all except 5-HT7R expressing vPNs, and V by all except 5-HT2BR expressing vPNs. Further, DM1 was not innervated by all except 5-HT2BR and 5-HT7R expressing vPNs. In addition, glomeruli DM4, DC4, VM6, VL2p, DA3, DP1l, DP1m, VC3m, and VL2a were not innervated by a combination of two 5-HTR expressing vPN types. As for glomerulus not innervated by a single 5-HTR expressing vPN, 5-HT2AR expressing vPNs did not innervate six glomeruli (DL2d, VA1v, VC1, VL1, VM4, and VM5) while 5-HT2BR and 5-HT7R expressing vPNs likely did not innervate DM2 and DL3, respectively. Analyzing the plane of preference that lacked 5-HTR expressing vPN innervation, we found that 5-HT7R expressing vPNs were unlikely to innervate glomeruli in the anterior regions (DA3, DL3, DL4, and VL2a) while 5-HT1AR, 5-HT1BR, and 5-HT2AR expressing vPNs were unlikely to innervate glomeruli in the posterior regions (DM1 and VM1).

We next analyzed LH regions innervated by each 5-HTR vPNs. This analysis proved to be difficult as the innervation of vPN in the LH is a collection of multiple vPN cell bodies from the AL. We can conclude that 5-HTR expressing e-vPNs and i-vPNs enter from different angles into the LH. 5-HTR expressing e-vPNs enter from a dorsal region coming downwards (Figure 7A, 7B, and 7D, green arrowhead) while 5-HTR expressing i-vPNs enter the LH from the dorsal regions (Figure 7A, 7C, and 7E, purple arrowhead). In terms of plane preference, 5-HTR expressing e-vPNs tend to stay with the dorsal lateral regions while the 5-HTR expressing i-vPNs stay within the ventral region but can occasionally spread out throughout the LH.

The MCFO analysis informs us of the characteristics of both 5-HTR expressing e-vPN and i-vPN glomerular innervation, odor valence, and plane preference. However, it could not predict a single or a combinatorial 5-HTR expression within a neuron or a subpopulation since each expression is obtained at random. I, therefore, sought to identify more restrictive driver lines that can provide consistent and sparse vPN expression as another means to determine 5-HTR receptor logic within the 5-HTR expressing vPNs.

Two subpopulations of i-vPN express distinct 5-HTR profiles and innervation patterns.

We searched the FlyLight database (Jenett et al. 2012) for candidate driver lines that included a small number of vPNs as the only neurons in the AL as another means to determine if vPNs that innervate different regions of the olfactory system also express different 5-HTRs. Out of the total 7,000 transgenic lines, we found 7 candidate vPN lines; R24H08, R30A10, R32F06, R76H03, R77C09, R80B05, and R86G06. Out of the five, we selected LexA driver lines of R24H08 and R86G06 for 5-HTR expression analysis because they possess a low vPN count, distinct innervation patterns, and little innervation from other neurons in the brain.

Using the vPN-LexA lines, 5-HTR-Gal4-T2A-Gal4-MiMIC lines, LexAop-GFP and UAS-RFP, we created a cross that can drive the expression of one fluorophore in our i-vPNs and a different fluorophore in all the neurons that express a given 5-HTR. Within R24H08-LexA and R86G06-LexA (R86G06-Gal4 does express OSN), the i-vPNs are the only cells that innervate the AL (Figure 8A and Figure 8B), making these driver lines excellent for studying i-vPNs. We found that R24H08-LexA i-vPNs densely innervate two glomeruli; DC3 (100%, n= 9 brains) and VL2a (100%, n=9 brains) while sparsely innervating the VC2 glomerulus (89%, n=9) (Figure 8C). These glomeruli respond to attractive (DC3 and VL2a) and neutral odors (VC2).

Meanwhile, R86G06-LexA i-vPN (n= 7 brains) innervate 30 glomeruli in the AL. Out of the total, 17 glomeruli respond to attractive odors (From highest, DC4, VA7m, VM5, DL2v, VA2, DM4, DP1m, DP1l, DL2d, VM7, VA1v, VM2, VM3, DA3, DM6, VM4, VA1d), seven to aversive odors (from highest, DC2, VA3, VA7l, DL1, D, DL5, and DA2) and six to neutral odors (From highest, VC1, VC2, DC1, DM2, VA4, DM5). R86G06-LexA did not innervate 18 glomeruli, eight being attractive (DC3, DL3, DM4, VA6, VL1, VL2a, VL2p, and VM1), five aversive (DA1, V, VA5, VC3l, and VC3m), and four neutral (DA4, DL4, and DM1). From a plane preference, R86G06-LexA expand throughout all planes and depth of the AL (Figure 8C).

In the LH, both i-vPN subpopulations occupy posterior regions. However, R24H08-LexA axons innervate mostly the ventral region (in the midline, R24H08 has a component that projects dorsally) (Figure 8D and 8F) while R86H08 axons innervate the dorsal region (Figure 8E and 8G). Both subpopulations do not include the same neurons nor do they overlap greatly in the AL, or at all in the LH (Figures 8I and 8J).

Next, we were interested in identifying the serotonin receptors expressed by each set of i-vPNs. Interestingly, we found that all R24H08-LexA i-vPNs only express 5-HT1A and 5-HT1B receptors while all R86G06-LexA i-vPNs only express 5-HT7Rs (Figures 9 and 10). Thus, two populations of i-vPNs innervating different glomeruli and LH zone have a non-overlapping 5-HTR expression (Figure 11).

Potential effects of RNAi knockdown of i-VPN lines on odor-guided behavior.

Knowing that R86G06-Gal4 i-VPNs only express 5-HT7R, I sought to determine the effects of RNAi-knockdown of the 5-HT7R in R86G06 i-VPNs on fly odor-guided behavior. We conducted a T-maze two-choice assay which determines the choice preference towards a selected odor after genetically reducing 5-HT7R expression in the R86G06-Gal4 line. Then, we would calculate the performance index based on the total flies occupying an odor chamber (Figure 12A). All R86G06-LexA i-VPN images innervate two glomeruli, the aversive DC2, and the attractive DC4. We selected the odor 1-octen-3-ol, a DC2 glomeruli odor that has a reported performance index of about -0.4 (Knaden et al. 2012). We compared our experiment with four different controls as well as two different odor concentrations, 1:1000 and 1:2000 (Figure 12B), however, observed no significant effects of 5-HT7 RNAi on aversion to 1-octen-3-ol.

We theorized that the T-maze itself may not be suitable for 1-octen-3-ol due to the volatile nature of the odorant. We tested aversion to 1-octen-3-ol using another behavior assay with a similar principle as the T-maze assay. Here, the odor is contained in an agarose droplet within a petri dish and the fly is allowed to roam inside the arena (Figure 12C), however again, we found also no significant effect of expressing the 5-HT7-RNAi in the R86G06-Gal4 line (Figure 12D).

Discussion:

Neuromodulation allows a neuron within a circuit to have great flexibility when coding sensory information. Such a mechanism is very important in the olfactory system since odorants are plentiful, existing in different ecological environments, concentrations, mixtures, and contexts. The above factors are further complicated by the internal state of the animal which changes according to its satiety and arousal states (reviewed in Oram and Card 2022). The correct representation of this information is valuable for the animal to survive. For example, CO₂ can provide the context of a food source or danger. When a fly is in a “foraging” state, the pathways that promote attraction are activated. On the contrary, when the fly is not foraging, the attraction is silenced while avoidance pathways take the animal away from the source. This behavior is facilitated by different OSN receptor types which bind onto the same odor and activate different glomeruli in dedicated behavior response circuits (Jones et al. 2007; Ai et al. 2010; van Breugel et al. 2018). Furthermore, fly larvae and adults have different responses to the odors coming from *Leptopilina* parasitic wasps. Targeting the OR49a receptors, these odors would elicit a strong avoidance in fly larvae and reduced oviposition by female adults within these areas (Ebrahim et al. 2015). Knowing that behavioral responses operate through dedicated circuits, neurons express that neuromodulatory components can regulate circuit activity through increasing or decreasing responses when stimuli are combined with various contexts. Neuromodulation increases the behavioral flexibility of the animal to allow greater behavioral success in the environment.

Our study aimed to understand the role of 5-HTR receptor diversity within a population that relays information from the first-order to second-order olfactory centers. i-vPNs are mostly known as GABAergic projection neurons that follow the mALT tract to the LH (Jefferis et al. 2007: 20; Liang et al. 2013; Strutz et al. 2014). The behavioral implications of i-vPNs could be understood through previous research on the GABAergic MZ699-Gal4 population. The Parnas model suggests that i-vPN play a role in facilitating presynaptic inhibition of the mALT ePNs in the AL. At low OSN spiking thresholds, a release of GABA by i-vPNs into the dendritic regions of the AL would generate a high-pass filter which causes discriminatory selection of odorants by food-related ePNs (Parnas et al. 2013). Other the other hand, the Liang model suggests that food-related odorants activate i-vPN to release inhibitory signals to suppress the activity of food-associated LHN targets while allowing the passage of information from pheromone-associated ePNs to its downstream targets. This feature, described as parallel inhibition, allows i-vPNs to inhibit specific olfactory-processing channels while allowing simultaneous entry of excitatory output of ePNs into the LH (Liang et al. 2013). Such a mechanism allows for olfactory information encoding of different biological values (Food vs. Mating) to be regulated according to the context currently experienced by the animal. Further, ePN and i-vPN of the MZ699-Gal4 population receive similar information from OSNs in the AL but have opposite actions in the lateral horn (Wang et al. 2014). In addition, some i-vPNs were known to electrically couple with ePN, which could provide i-vPN-ePN cross-talk across selected glomeruli together with causing postsynaptic inhibition to their downstream targets (Wang et al. 2014). Moreover, the Strutz

model divides the MZ699-Gal4 i-vPN into two subgroups based on their innervation patterns in the AL and LH as well as their functional role. When an attractive odor is detected by i-vPNs, GABA release of MZ699-Gal4 i-vPN causes postsynaptic inhibition of vIPr neurons, refining the representation of attractive odors in the LH (Strutz et al. 2014). They also showed that silencing i-vPN activity causes an aversion to attractive odors in a two-choice behavioral assay. According to Ca^{2+} imaging responses, Strutz et. al also separated the LH into three different zones that code odor intensity and hedonic valence. While the LH-PM (Lateral horn-posterior medial zone) and LH-AM (Lateral horn-anteromedial zone) innervating i-vPN both encode odor intensity, the LH-PM expressing i-vPNs are activated across multiple odor concentrations while the LH-AM innervating vPNs are activated by a higher odor concentration from distinct odorants (Strutz et al. 2014). Altogether, MZ699-Gal4 i-vPNs regulate different effects based on its presynaptic and postsynaptic targets, innervate differently within the AL and LH, and encode different roles in the LH to facilitate behavior.

MZ699-Gal4 i-vPNs express around 51 vPNs (Liang et al. 2013; Parnas et al. 2013; Strutz et al. 2014). However, recent studies have shown that the GABAergic mPN population expands to about 71 neurons (Bates et al. 2020) suggesting that MZ699 only informs us about a subset of i-vPNs instead of being a representation of the whole population (described in Bates et al. 2020; Coates et al. 2020). Uniglomerular cholinergic PN (ePN) were previously described to be divided into two AL cell clusters, adPNs and latPNs of the AL, which release cholinergic input into LH and the MB (Jefferis et al. 2007: 200; Li et al. 2017). From this study, I would add the cluster of cholinergic vPNs to this group. To clarify the nomenclature, we identify these ventral neuron clusters as e-vPNs and i-vPNs based on their morphology and major neurotransmitter content. Uniquely, both cell populations express all insect 5-HTRs and indicate signs of 5-HTR co-expression (Sizemore and Dacks 2016).

I found that 5-HTR co-expression does indeed exist within both e-vPN and i-vPN populations. This is done by combining two driver lines that contain a total 5-HTR population and observing potential co-expression in the cell bodies. The data was not fully comprehensive as we encountered issues with the three 5-HTR-LexA driver lines that did not share similar expressions with our verified 5-HTR-T2A-GAL4 lines. Interestingly, there are common trends shared by both vPN lines. First, co-expression of the 5-HT2B-LexA is similar between both vPN clusters (i-vPN = 40% while e-vPN = 43%). 5-HT7R has the highest binding affinity toward serotonin, typically causing excitation via the PKA pathway (Nichols and Nichols 2008; Gasque et al. 2013). As the concentration of 5-HT increases, 5-HT2BR has the next lowest binding affinity and likely causes an excitatory response via the IP3 pathway. The facilitation of two separate pathways enables a rapid response of 5-HT release, likely facilitating a change in the activity of vPNs that express given receptors. The coupling of an excitatory 5-HTR (5-HT2AR, 5-HT2BR, and 5-HT7) with an inhibitory 5-HTR (5-HT1AR and 5-HT1BR) may result in a concentration-dependent involvement of 5-HT modulation within a circuit. Such a mechanism may be analogous to how an

attractive odor becomes aversive to an animal when there is a change in odor concentration and internal state (Semmelhack and Wang 2009; Devineni et al. 2019).

Next, the difference in 5-HTR type coupling would lead to different consequences of effect within a cell. Activation of the negatively coupled 5-HT_{1R} would lead to reduced cell activity through the PKA pathway, while activation of 5-HT_{2R} and 5HT₇ would induce excitation through recruiting the IP₃ and PKA pathways, respectively (Nichols and Nichols 2008; Johnson et al. 2009; Tierney 2018). If a cell expresses only inhibitory 5-HT receptors, inhibition of the neuron could occur over a longer period and at different concentrations of 5-HT, similar to what could be 5-HTRs that express excitatory receptors. In addition, excitatory 5-HTRs in insect targets two different secondary messenger pathways, allowing for a greater excitatory effect due to more activated cellular components. Other the other hand, expressing both excitatory and inhibitory receptors allow for a period of excitation followed by inhibition, assuming 5-HT_{1R} has lower binding affinities than the 5-HT_{2R} and 5-HT_{7R} (Gasque et al. 2013). While dual modulatory-receptor expression of two 5-HTRs is less known, this mechanism can function to regulate different behavioral outcomes. Histamine and GABA co-expression in the tuberomammillary nucleus (TMN) was known to regulate wakefulness in mice where the tonic release of GABA causes inhibition of the animal's arousal state (Yu et al. 2015). When GABA release is inhibited in the cell, the animal experiences more locomotor activity, and wakefulness. Through understanding how vPNs express a given 5-HTR, my thesis gives an idea of how combinations of 5-HTR expression promote other functional roles in behavior.

To understand if the processing of certain odors by vPNs is more likely to be affected by a given 5-HTR, we determined where 5-HTR expressing e-vPNs and i-vPNs innervate using the MCFO technique. We discovered a greater expression of the e-vPN in multiple 5-HTR populations (5-HT_{1AR}, 5-HT_{1BR}, 5-HT_{2AR}, and 5-HT_{2BR}) while a greater expression of i-vPNs for the 5-HT_{7R}. The 5-HTR expressing e-vPNs-equally innervate both attractive and aversive encoding glomeruli while the i-vPN mostly innervate glomeruli encoding attractive odors. The attractive odors encoded by i-vPNs included glomeruli responsive to acetic acid (DC4, DP1m, and DP1l), supporting previous research that the MZ699-Gal4 population is responsible for mediating attractive odors (Liang et al. 2013; Strutz et al. 2014). As a consequence, the 5-HT_{1R} and 5-HT_{2R} could provide both excitatory and inhibitory input to e-vPN, regulating cholinergic activity in the MB and LH while 5-HT_{7R} regulation would promote GABA release by i-vPNs, increasing inhibition of its downstream LHN targets.

The 5-HTR expressing vPNs innervated glomeruli in a combinatorial manner, some innervating one glomerulus while other glomeruli were innervated by multiple vPNs expressing different 5-HTRs. Four glomeruli are innervated by vPNs from all five 5-HTR-T2A-Gal lines, of them three were attractive, two were aversive, and one responds to both behaviors. The top 15 glomeruli innervations by each 5-HTR expressing responding to attractive odorants are related to citrus fruit (farnesol), fragrant aromatics (eugenol), and amines (pyrrolidine). The aversive glomerulus responds to 4-methyphenol which is

commonly found in fecal matter. These odors are important for food-searching, mate-searching, and egg-laying behavior (Min et al. 2013; Mansourian et al. 2016; Chin et al. 2018; Haq et al. 2018). Taking all the information together, we predict that vPNs that express the 5-HT7R generally are involved in the processing of attractive odors while the other 5HTRs appear to be involved in both attractive and aversive odor responses that influence food-searching, mate-searching, and oviposition activity in an odor-rich environment.

The MCFO matrix (Figure 5) helped us analyze the glomerular targets of each 5-HTR expressing vPN and help us compare the difference between e-vPNs and i-vPNs targets. The glomerular maps (Figure 6) allowed us to compare the percent expression of 5-HTR expression in each glomerulus to enable us to identify regions of possible 5-HTR co-expression by each 5-HTR vPN. The MCFO approach comes with a few caveats. First, MCFO has a bias of expressing only vPNs that have the highest expression of a given 5-HTR. Next, when both e-vPNs and i-vPNs were expressed in an AL, their innervation within each glomerulus could not be distinguished from each other. Only innervations that can be observably traced into its vPN cell body and its associated tract (mIALT or mALT) were counted as positive innervation. Finally, we did not count in clones that had an obstruction from non-vPN neurons entering the AL (LNs and other PN types). Overall, this study shows that vPNs expressing each 5-HTR innervate different regions of the AL and LH. In particular, 5-HT7R expressing vPNs show different glomerular targets than the other four 5-HTR subtypes. This suggests 5-HTR subtypes are expressed to take on different roles in olfactory processing.

We explored 5-HTR expression in two specific populations of i-vPNs, those expressed by the R24H08 and R86G06 driver lines. In general, both populations innervate glomeruli that respond to attractive odorants. However, both i-vPN populations also innervate glomeruli that respond to aversive odorants. For example, R86G06-LexA innervates seven aversive glomeruli with five glomeruli having a percent innervation from half of the total population (DC2, VA3, VA7I, DL1, and D) while R24H08-LexA innervates VC2 which response to both attractive, aversive, and neutral stimuli. Our findings may suggest two things; 1) i-vPNs obtain information from aversive glomeruli to affect attractive behavior or 2) i-vPNs can affect both attractive and aversive behaviors. Next, we showed that these two i-vPN subgroups project into different regions of the lateral horn, the R86G06 representing a dorsally projecting i-vPN subpopulation while the R24H08 represents a ventrally projecting i-vPN subpopulation (Marin et al. 2002). Interestingly, R86G06-LexA showed similar LH innervations with LH-PM i-vPN which responds to the same glomeruli DM2, DM4, VM5, and VM7 (Figure 8C) while R24H08-LexA show similar LH innervation with LH-AM i-vPNs and target the same glomerulus DC3 (Figure 8C, Strutz et al. 2014). However, these i-vPN subpopulations innervate glomeruli that respond to aversive odors when previous papers only described their roles in mediating attractive odors (Liang et al. 2013; Parnas et al. 2013; Strutz et al. 2014). We suggest that the MZ699-Gal4 likely drives the expression of only a subset of the total i-vPN population.

In terms of 5-HTR expression, R86G06-LexA expresses only the excitatory 5-HT7R while R24H08-LexA expresses two populations of 5-HTRs, 5-HT1A, and 5-HT1B. Based on the Strutz model, the release of GABA produces more attraction, thus 5-HT7R activation would cause more GABA release into the environment, increasing attraction. On the contrary, 5-HT1A/1B activation would facilitate more aversion because activation of one or both 5-HTR would inhibit the release of GABA into the LH regions. Therefore, in the presence of a given odor, RNAi targeting of 5-HT7R would result in less attraction while 5-HT1A/1B RNAi would induce a more attractive response in behavior. Increased attraction from targeting vPNs from 5-HT1AR-RNAi experiments (Auda 2017, unpublished). When 5-HT1AR in MZ699 was reduced, i-vPN can release GABA into its downstream targets, increasing its attraction to apple cider vinegar. Taken together, studying two subpopulations of 5-HTR expressing i-vPNs verified that a combinatorial pattern of 5-HTR expression exists in a population. However, I would like to add that these i-vPNs are capable of processing both attractive and aversive information.

Finally, we wanted to determine the consequence of the 5-HT7R knockdown on the odor-guided behavior of the R86G06 i-vPNs. Interestingly, R86G06-Gal4 responds strongly activates the odor 1-octen-3-ol (Julius Jonaitis, unpublished), an aversive compound in a mold that disrupts dopamine packaging in drosophila causing neuron degeneration (Inamdar et al. 2013). This odor is detected by Or13a and processed in the DC2 glomeruli. We hoped by conducting a 5-HT7R knockdown in the R86G06-Gal4 population, we would observe an impact on the aversive response to 1-octen-3-ol. We were not fortunate to obtain any significant data from our behavior experiments. Our experimental and control animals displayed a variability that results in almost neutral responses. It could be arising from two factors; 1) the odor is very volatile and spreads too quickly in a closed chamber, 2) the odor has a state-dependent context (i.e., mediated by satiety or arousal), and 3) there are populations of neurons other than R86G06 i-vPNs that encode aversion to 1-octen-3-ol and the 5-HTR knockdown was not sufficient to create a substantial impact. We also observed that during the fly arena assay that one fly trial showed a difference individual preference towards 1-octen-3-ol. Some flies are attracted to the odor-associated zone while some flies are aversive to it. In our experiment, we worked with starved flies, assuming that 1-octen-3-ol is involved in food-searching behavior. It could be that such odors may have greater importance in other behaviors like egg-laying and courtship.

In conclusion, we found that vPNs expressed a combinatorial pattern of all 5-HTRs. We then identified categorized these vPNs into two groups, the e-vPNs, which respond to both attractive and aversive odor glomeruli, and i-vPNs which respond to mainly attractive responding glomeruli. Next, we also showed that 5-HT7R most likely co-express with the 5-HT2BR in both e-vPNs and i-vPNs subgroups. We also found three groups of 5-HTR expressing vPN innervation patterns using MCFO; 1) 5HT1A and 5-HT1B, 2) 5-HT2A and 5-HT2B, and 3) 5-HT7. Further, we found that 5-HT7 has the most sparse glomeruli innervation in the AL. Finally, we demonstrated two populations of i-vPNs that express distinct 5-HTR expression as well as glomerular and LH innervations that complement and further elaborates their roles in regulating odor responses in the LH. My study provides a foundation to explore 5-HT modulation in populations that express all 5-HTR types and how such expression affects odor processing within two olfactory regions.

LIST OF FIGURES

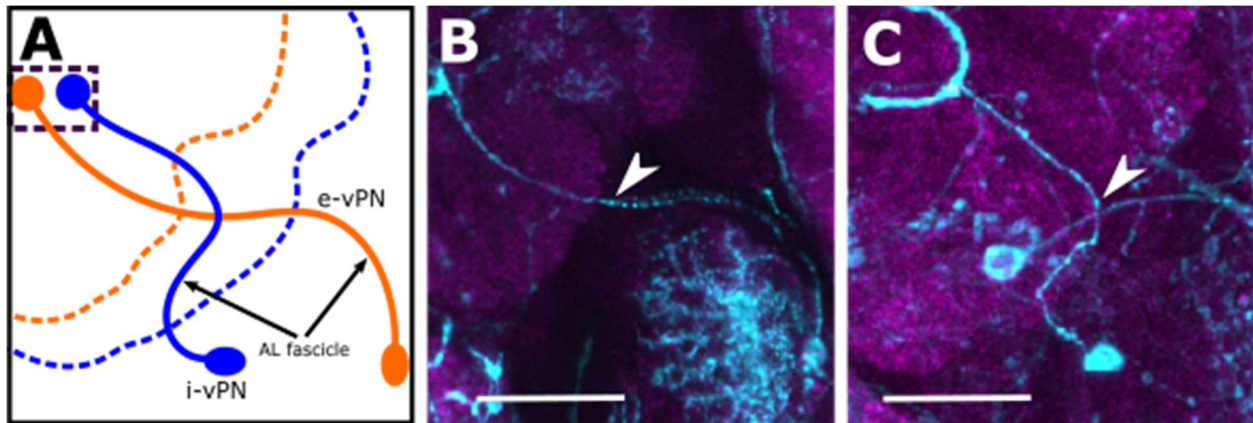


Figure 1. Morphology of vPN entering the AL through multiple AL fascicles.
A) Schematic showing vPN morphology within the AL. Blue lines represents i-VPNs while orange lines represents e-VPNs. Dotted lines represent the border of the AL. e-VPN clusters are slightly posterior than the i-VPN cluster hence the different color representation of dotted lines. The square dotted box represents the area where vPN dendrites collect and project out to the higher processing regions.
B) Confocal image of a e-vPN expressed using the MCFO technique (refer Methods). Arrowhead represents an AL fascicle. Scale bar is 20 µm.
C) Confocal images of an i-vPN expressed using the MCFO technique. Arrowhead represents an AL fascicle. Scale bar is 20 µm.

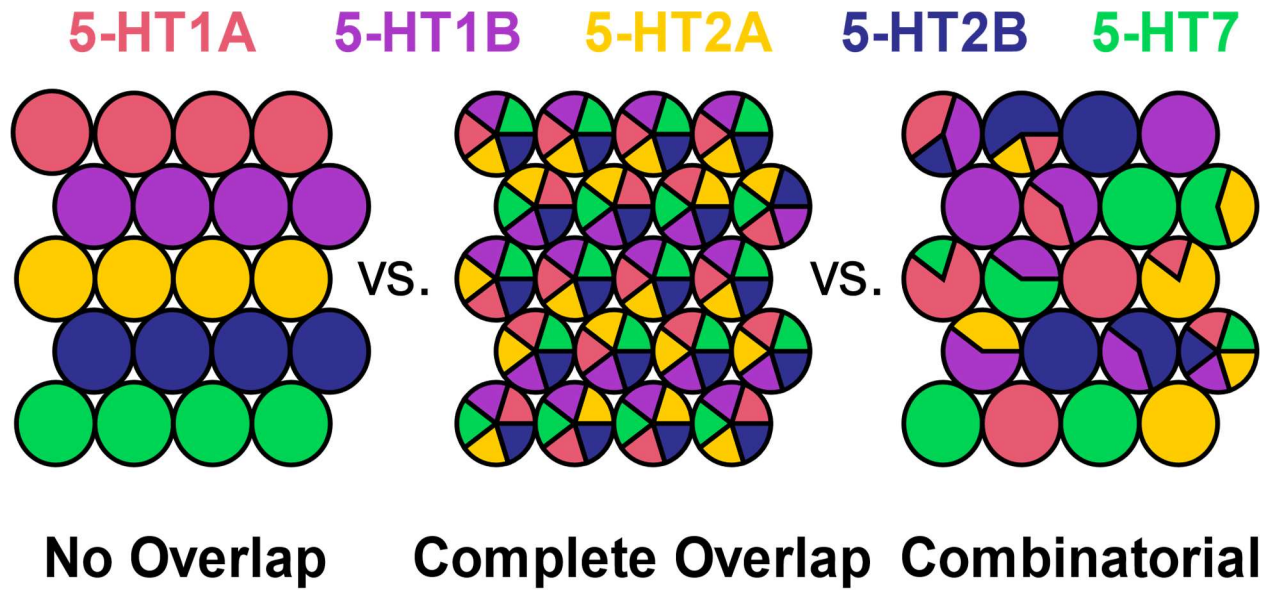


Figure 2. Schematic diagram of predicted 5-HTR expression within the vPN population. From left, vPN could express only ONE 5-HTR at a time, express ALL 5-HTR at a time (middle) OR express a combination between one to all 5-HTR subtypes

A % Co-expression

	5-HT1AGal4	5-HT1BGal4	5-HT2AGal4	5-HT2BGal4	5-HT7Gal4
5-HT2B-LexA	30% ± 4.42 (7.5)	13% ± 1.22 (7)	N/A	100% (7)	40% ± 4.4 (8.5)
5-HT7-LexA	31% ± 3.1 (9.5)	15% ± 2.5 (8)	N/A	N/A	100% (6.5)

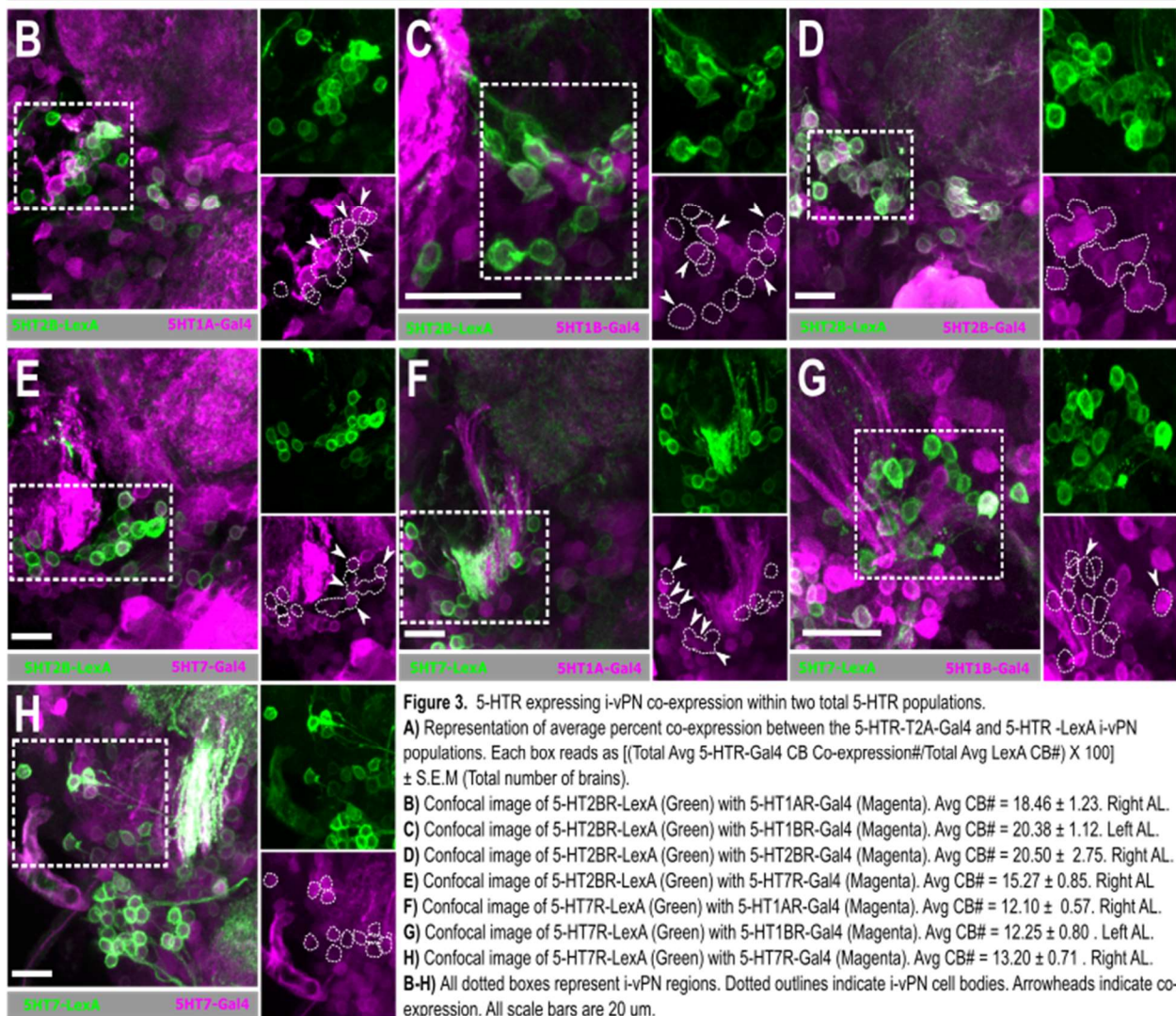
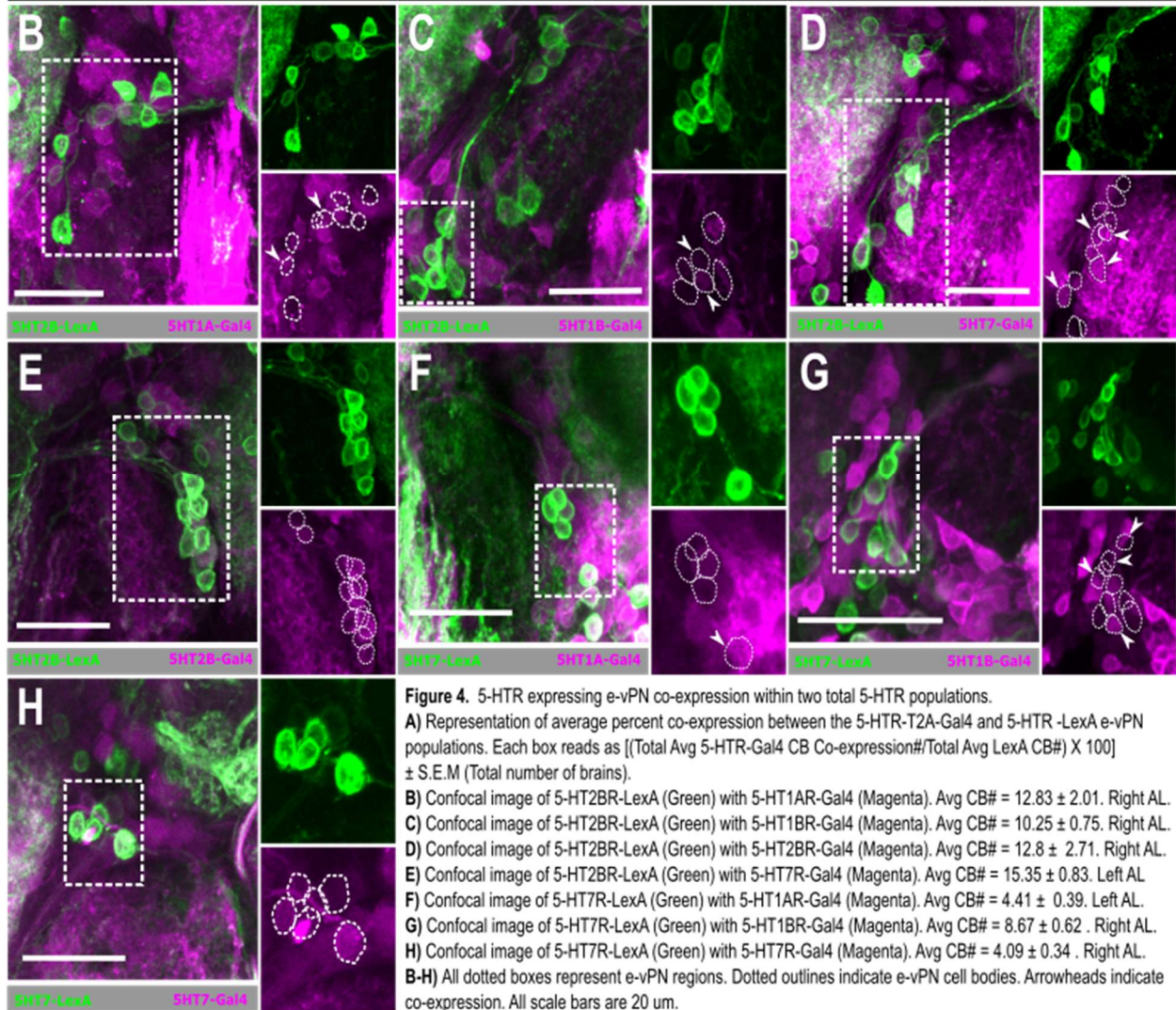


Figure 3. 5-HTR expressing i-vPN co-expression within two total 5-HTR populations. A) Representation of average percent co-expression between the 5-HTR-T2A-Gal4 and 5-HTR -LexA i-vPN populations. Each box reads as [(Total Avg 5-HTR-Gal4 CB Co-expression# / Total Avg LexA CB#) X 100] ± S.E.M (Total number of brains). B) Confocal image of 5-HT2BR-LexA (Green) with 5-HT1AR-Gal4 (Magenta). Avg CB# = 18.46 ± 1.23. Right AL. C) Confocal image of 5-HT2BR-LexA (Green) with 5-HT1BR-Gal4 (Magenta). Avg CB# = 20.38 ± 1.12. Left AL. D) Confocal image of 5-HT2BR-LexA (Green) with 5-HT2BR-Gal4 (Magenta). Avg CB# = 20.50 ± 2.75. Right AL. E) Confocal image of 5-HT2BR-LexA (Green) with 5-HT7R-Gal4 (Magenta). Avg CB# = 15.27 ± 0.85. Right AL. F) Confocal image of 5-HT7R-LexA (Green) with 5-HT1AR-Gal4 (Magenta). Avg CB# = 12.10 ± 0.57. Right AL. G) Confocal image of 5-HT7R-LexA (Green) with 5-HT1BR-Gal4 (Magenta). Avg CB# = 12.25 ± 0.80. Left AL. H) Confocal image of 5-HT7R-LexA (Green) with 5-HT7R-Gal4 (Magenta). Avg CB# = 13.20 ± 0.71. Right AL. B-H) All dotted boxes represent i-vPN regions. Dotted outlines indicate i-vPN cell bodies. Arrowheads indicate co-expression. All scale bars are 20 μm.

A	% Co-expression	5-HT1AGal4	5-HT1BGal4	5-HT2AGal4	5-HT2BGal4	5-HT7Gal4
5-HT2B-LexA		17% ± 4.3 (6)	24% ± 2.60 (8)	N/A	100% (7)	43% ± 3.0 (7.5)
5-HT7-LexA		25% ± 8.5 (6)	36% ± 7.61 (6)	N/A	N/A	100% (6.5)



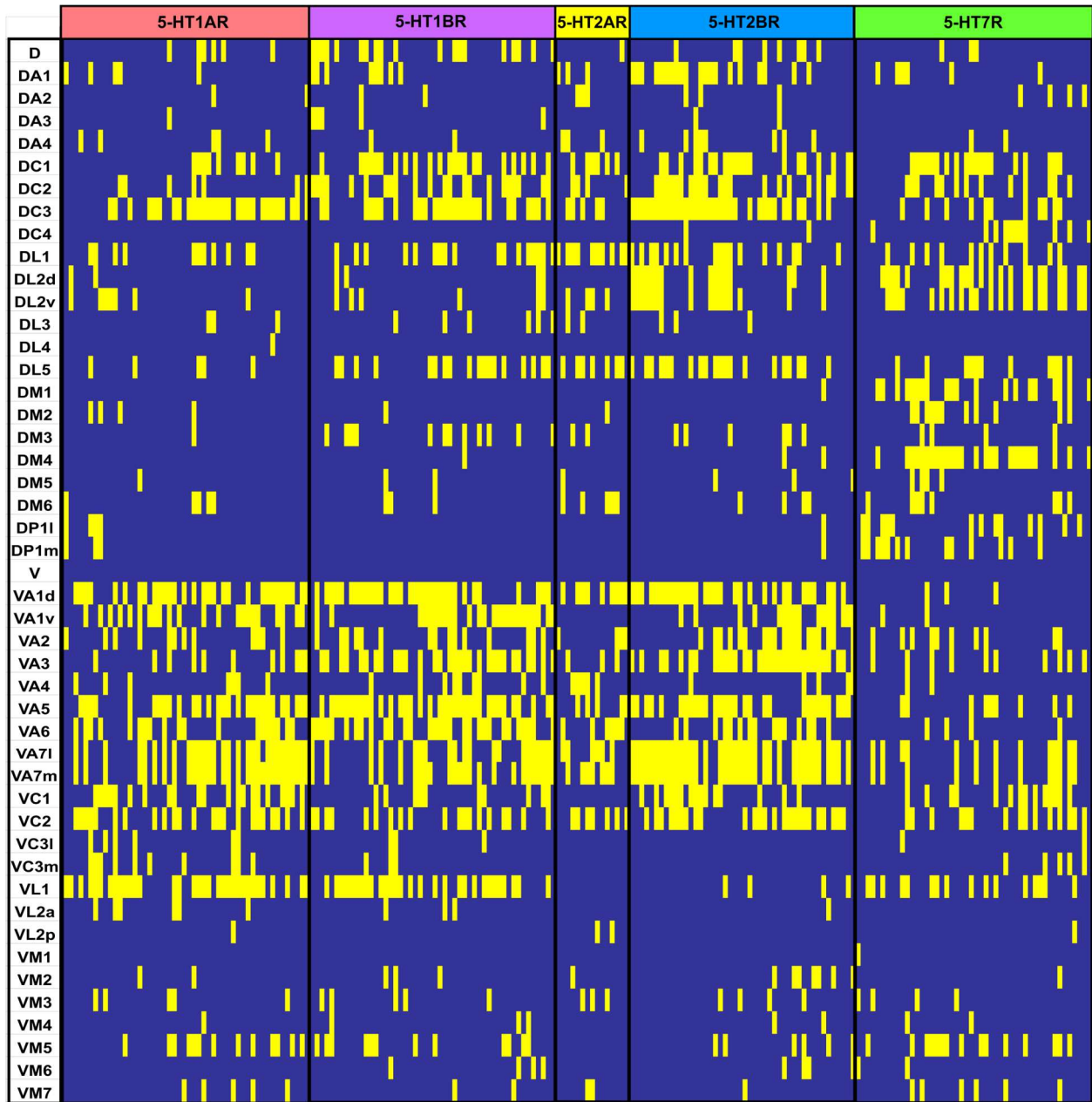
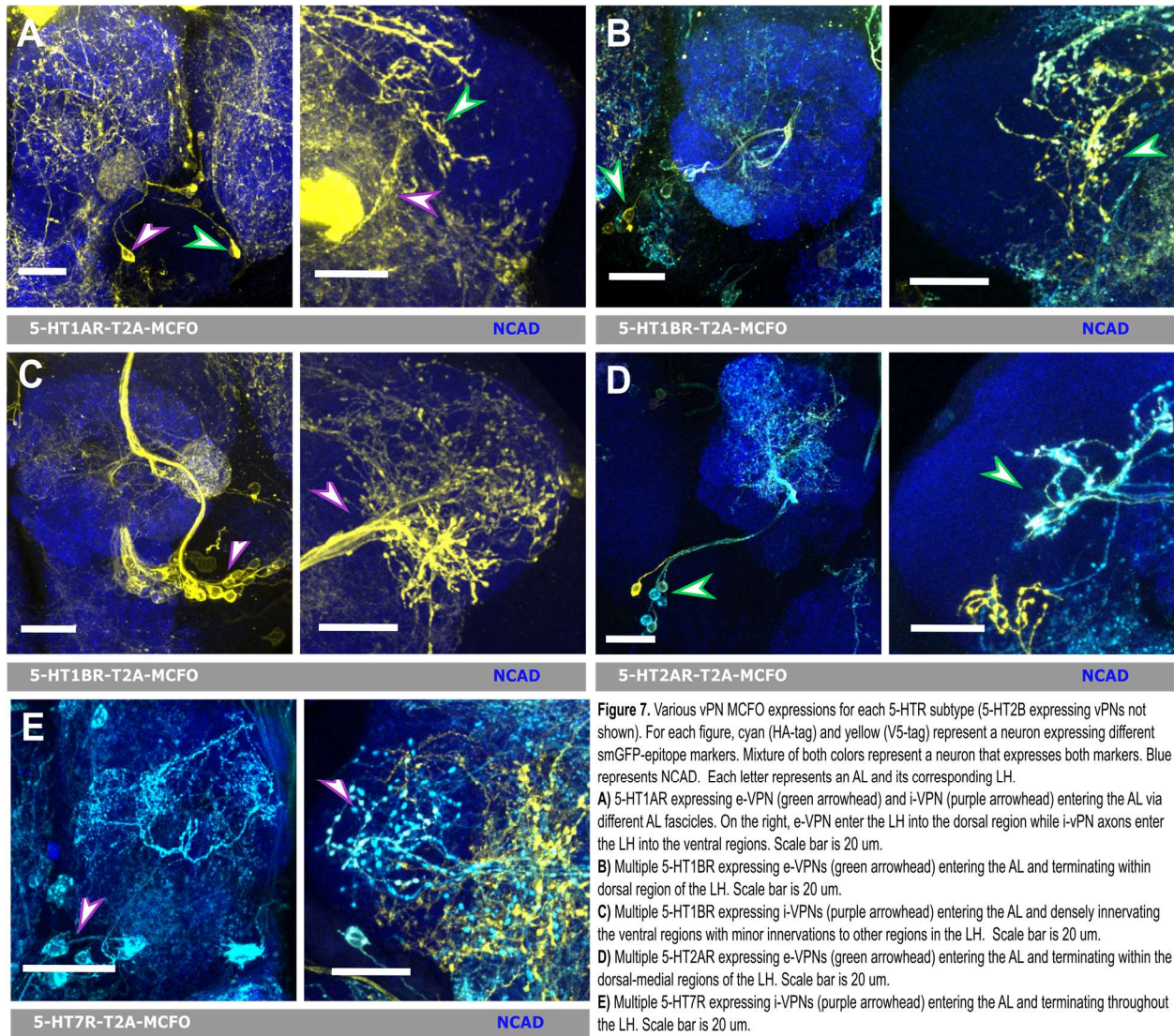


Figure 5. Representation of vPN glomerular innervation expressing each 5-HTR using MCFO. Each large column represents a 5-HTR population. Each single column represent a 5-HTR expressing vPN in a single AL (50 for 5-HT1AR, 50 for 5-HT1BR, 15 for 5-HT2AR, 46 for 5-HT2BR, and 48 for 5-HT7R). Each row represents an analyzed glomerulus. Yellow boxes represent positive innervations while blue boxes represent no innervations.



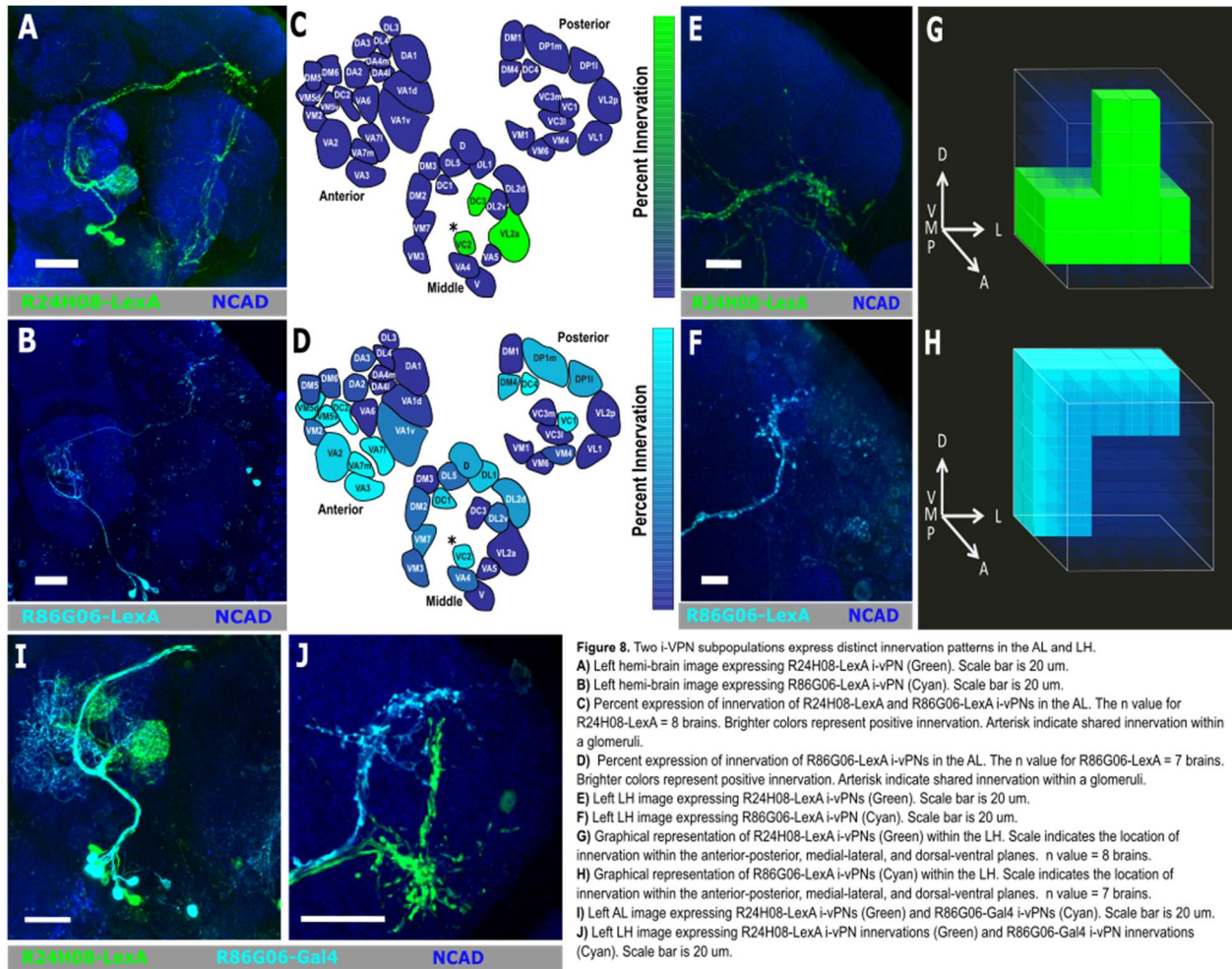


Figure 8. Two i-vPN subpopulations express distinct innervation patterns in the AL and LH. **A)** Left hemi-brain image expressing R24H08-LexA i-vPN (Green). Scale bar is 20 μ m. **B)** Left hemi-brain image expressing R86G06-LexA i-vPN (Cyan). Scale bar is 20 μ m. **C)** Percent expression of innervation of R24H08-LexA and R86G06-LexA i-vPNs in the AL. The n value for R24H08-LexA = 8 brains. Brighter colors represent positive innervation. Arterisk indicate shared innervation within a glomeruli. **D)** Percent expression of innervation of R86G06-LexA i-vPNs in the AL. The n value for R86G06-LexA = 7 brains. Brighter colors represent positive innervation. Arterisk indicate shared innervation within a glomeruli. **E)** Left LH image expressing R24H08-LexA i-vPNs (Green). Scale bar is 20 μ m. **F)** Left LH image expressing R86G06-LexA i-vPN (Cyan). Scale bar is 20 μ m. **G)** Graphical representation of R24H08-LexA i-vPNs (Green) within the LH. Scale indicates the location of innervation within the anterior-posterior, medial-lateral, and dorsal-ventral planes. n value = 8 brains. **H)** Graphical representation of R86G06-LexA i-vPNs (Cyan) within the LH. Scale indicates the location of innervation within the anterior-posterior, medial-lateral, and dorsal-ventral planes. n value = 7 brains. **I)** Left AL image expressing R24H08-LexA i-vPNs (Green) and R86G06-Gal4 i-vPNs (Cyan). Scale bar is 20 μ m. **J)** Left LH image expressing R24H08-LexA i-vPN innervations (Green) and R86G06-Gal4 i-vPN innervations (Cyan). Scale bar is 20 μ m.

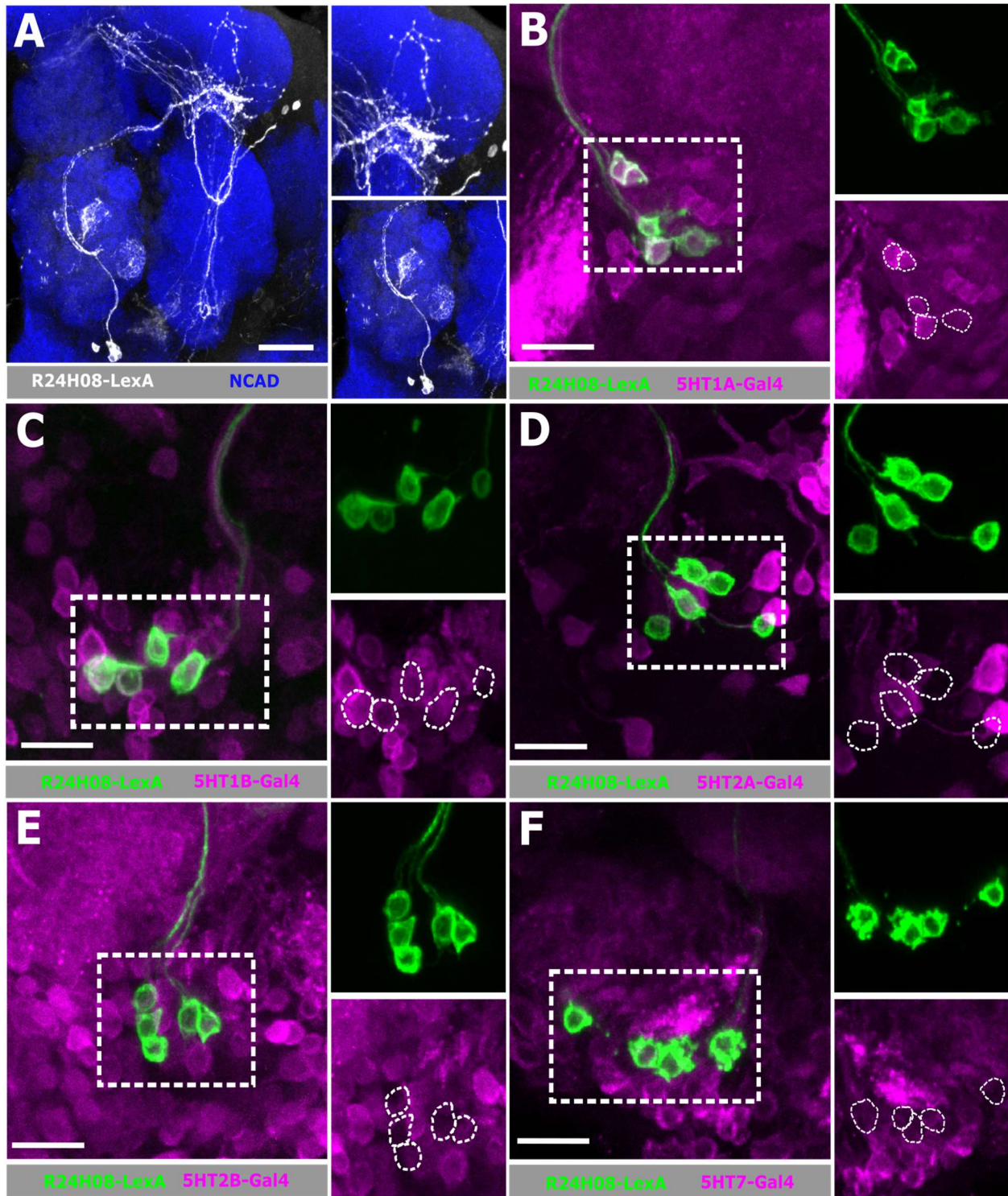


Figure 9. 5-HT expression of the R24H08-LexA i-vPN subpopulation.
A) Left hemi-brain image of R24H08-LexA i-vPNs (white). i-vPN projects into the AL via an AL fascicle and out to the LH via the mIALT. Note that there are other neurons within the LexA line on the right projecting into the LH. Blue indicates NCAD. Scale bar is 20 μ m.
B) 5-HT1AR expression (magenta) of R24H08-LexA cell bodies (green). Avg CB# = 4.79 ± 0.38 . N = 7 brains. Scale bar is 20 μ m.
C) 5-HT1BR expression (magenta) of R24H08-LexA cell bodies (green). Avg CB# = 4.71 ± 0.37 . N = 7 brains. Scale bar is 20 μ m.
D) 5-HT2AR expression (magenta) of R24H08-LexA cell bodies (green). Avg CB# = 4.94 ± 0.22 . N = 9 brains. Scale bar is 20 μ m.
E) 5-HT2BR expression (magenta) of R24H08-LexA cell bodies (green). Avg CB# = 5.17 ± 0.19 . N = 9 brains. Scale bar is 20 μ m.
F) 5-HT7R expression (magenta) of R24H08-LexA cell bodies (green). Avg CB# = 4.35 ± 0.23 . N = 10 brains. Scale bar is 20 μ m.
B-F) Dotted box indicate region of interest. Dotted lines indicate LexA cell bodies. Co-expression is indicated by a cell body with a white-green outline with a magenta body.

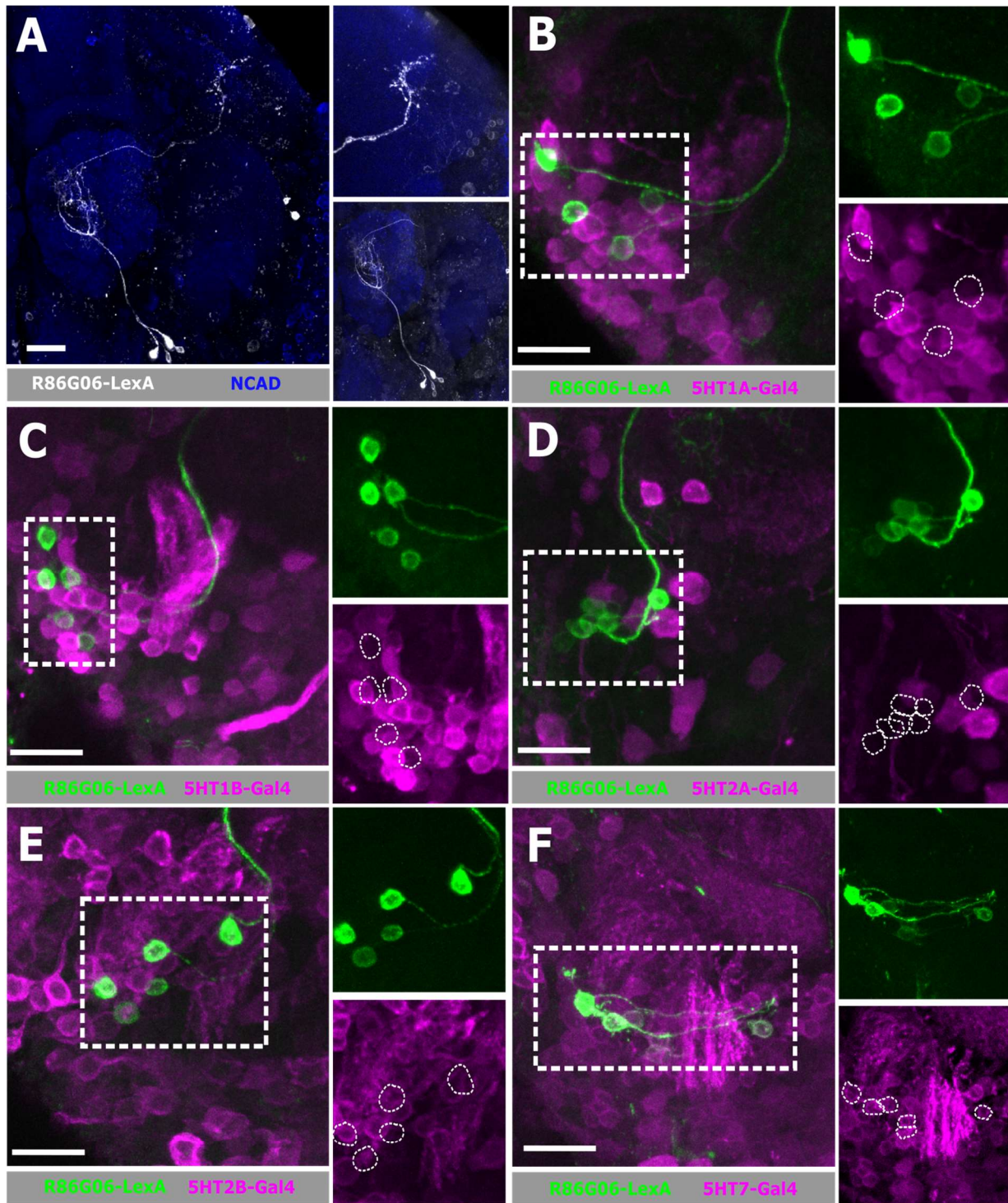


Figure 10. 5-HT expression of the R86G06-LexA i-vPN subpopulation.

A) Left hemi-brain image of R86G06-LexA i-vPNs (white). i-vPN projects into the AL via an AL fascicle and out to the LH via the mALT. Blue indicates NCAD. Scale bar is 20 μ m.

B) 5-HT1AR expression (magenta) of R86G06-LexA cell bodies (green). Avg CB# = 4.55 ± 0.11 . N = 7 brains. Scale bar is 20 μ m.

C) 5-HT1BR expression (magenta) of R86G06-LexA cell bodies (green). Avg CB# = 4.94 ± 0.20 . N = 7 brains. Scale bar is 20 μ m.

D) 5-HT2AR expression (magenta) of R86G06-LexA cell bodies (green). Avg CB# = 4.44 ± 0.18 . N = 9 brains. Scale bar is 20 μ m.

E) 5-HT2BR expression (magenta) of R86G06-LexA cell bodies (green). Avg CB# = 5.40 ± 0.18 . N = 9 brains. Scale bar is 20 μ m.

F) 5-HT7R expression (magenta) of R86G06-LexA cell bodies (green). Avg CB# = 4.40 ± 0.13 . N = 10 brains. Scale bar is 20 μ m.

B-F) Dotted box indicate region of interest. Dotted lines indicate Lex-A cell bodies. Co-expression is indicated by a cell body with a whitish-green outline with a magenta body.

5-HT Receptor Expression

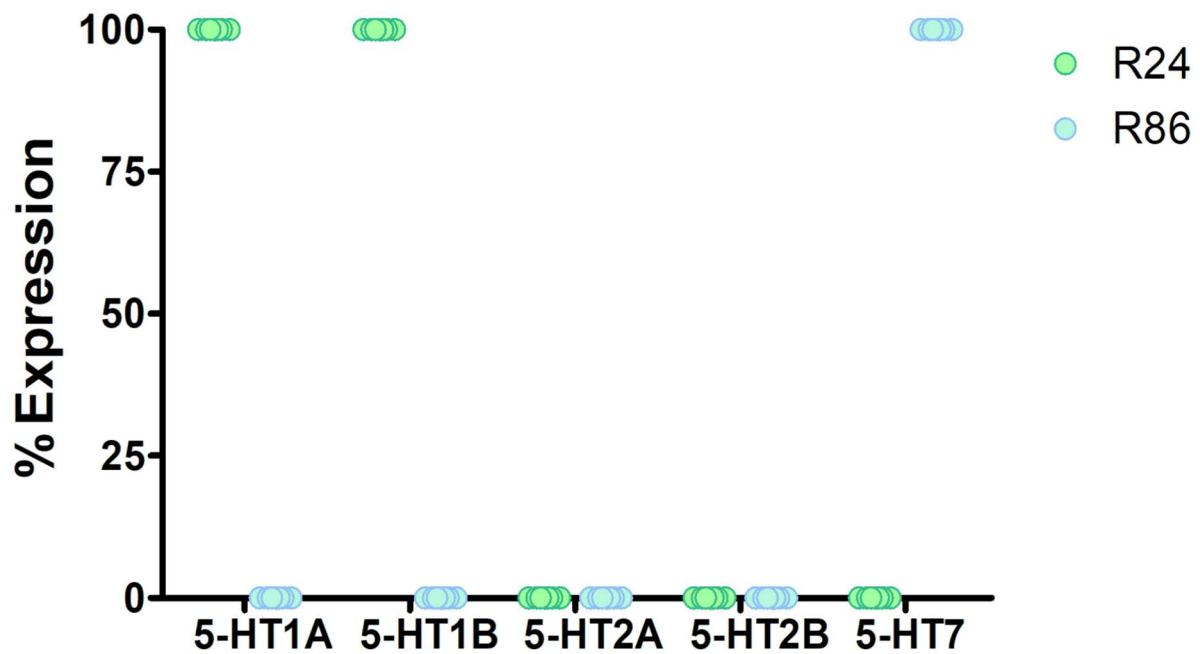


Figure 11. Graph representation of 5-HTR expression between two i-VPN populations, R24H08-LexA (Green) and R86G06-LexA (Cyan). The x-axis represent the 5-HTR types and y-axis represent percent co-expression. Each singular circle represents average percent LexA-5-HTR co-expression within a brain (i-VPN cell bodies for both AL). The n value for each i-VPN-LexA-5-HTR-Gal4 cross has been mentioned in Figure 9 and 10.

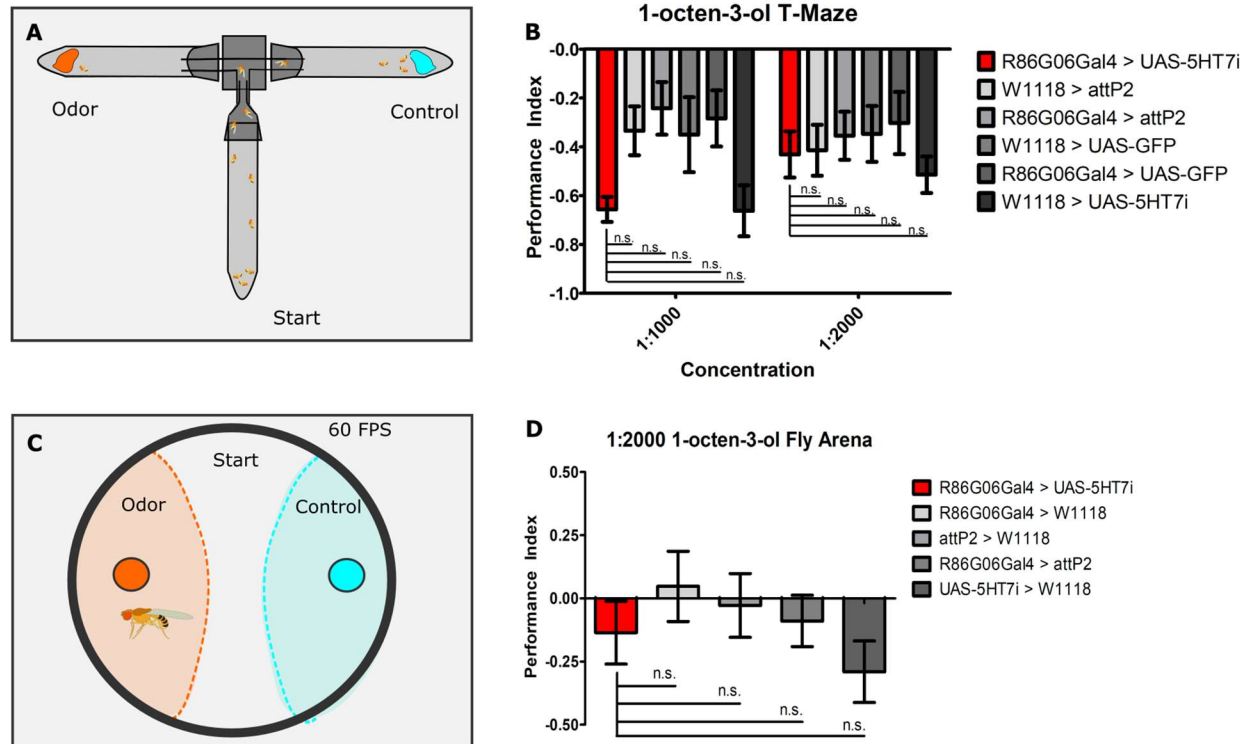


Figure 12. Two behavioral assays used to understand the consequences of R86G06-Gal4 i-vPN 5-HT7 knockdown on odor-guided behavior.

A) Schematic of the T-maze two-choice assay. Cold-anesthetized starved female flies were loaded into a start vial and allowed to make decision to climb to the odor-containing chamber (orange) or control-containing chamber (cyan, neutral odor). The performance index is calculated based on the number of flies in each chamber. Each t-maze contains 20-30 female flies.

B) Performance index for all tested genotypes at 1:1000 and 1:2000 1-octen-3-ol concentration. Each bar is an average of 12-15 T-maze runs for one experimental and five control genotypes. Data shows no significance.

C) Schematic of the fly arena assay. Starved flies were placed into a petri dish containing odor agar (orange) and control agar (cyan). One fly was placed at the start region and recorded at 60 FPS for 15 minutes. Each dotted line represents the predicted space an odor/ control would be occupying. The white space represents the neutral zone. Performance index is the total number of frames the fly spent its time within a zone.

D) Performance index of all tested genotypes at 1:2000 1-octen-3-ol concentration. Each bar is the average of 20 runs per genotype with one experimental and four control genotypes. Data shows no significance.

Chapter 3: Future Directions

My thesis used multiple transgenic tools and immunocytochemistry to determine organizational principles of the expression of multiple 5-HTRs by a single population of neurons in *Drosophila*. This anatomical approach helps us categorize the morphological patterns, receptor logic, and odor valence of vPNs that express different 5-HTRs which allows us to predict what 5-HTRs can affect responses to an odor. Further, I attempted to demonstrate the effects of the 5-HTR knockdown of a specific 5-HTR vPN population on odor-guided behavior. Even though unsuccessful, it provides us with useful troubleshooting guides when testing different types of odors in future experiments.

In chapter 2, I demonstrated that 5-HTR co-expression indeed exists within both the e-vPN and i-vPN populations, confirming the predictions of previous research (Sizemore and Dacks 2016). Understanding this idea and the morphology of vPNs, we wonder how are 5-HTRs expressed within a vPN neuron. Some questions are 1) If there is co-expression, do 5-HTRs dimerize into one unit or are they localized to specific olfactory centers (AL and LH)? 2) Are there differences in 5-HTR ratios between receptor types and 3) are the CSDns connected to processes within the AL or together with the LH? These questions would help us appreciate the diversity of neuromodulation methods in providing the best outcome of behavior in an odor-rich environment. I believe that these questions could be answered through transgenic tools that can label synaptic connections (i.e., GRASP), molecular screening on 5-HTRs, and testing the effects of one 5-HTR type versus the other in behavior.

My next transgenic methods using MCFO demonstrated that vPNs also play an important role in understanding 5-HTR diversity. Since four out of five 5-HTR types express mostly e-PNs (5-HT1AR, 5-HT1BR, 5-HT2AR, and 5-HT2BR), we can't deny that both populations can display 5-HTR co-expression to modulate their cell activity. Then, we wonder, how do we differentiate these populations besides comparing their morphology? MCFO likely highlights vPNs with the highest level of 5-HTR expression, therefore it may not account for all individual PNs that express a given vPN. In addition to innervating both LH and AL, we wonder if odor processing is different in e-vPNs in comparison with i-vPNs. Contrary to ePN which is mostly uniglomerular, e-vPNs are multiglomerular and project to the MB calyx before the LH. This cluster could be used to study odors important in associated learning. e-vPN roles in the MB may differ as this cluster responds to broad ranges of odor stimuli as well as regulate odor response based on experience and context compared to its ePN counterpart which responds to specific odors (Jefferis et al. 2007; Stensmyr et al. 2012b). Next, we found out that 5-HT7 is sparsely expressed

throughout the AL. Since this 5-HTR is excitatory and has a strong binding affinity to 5-HT (Gasque et al. 2013), we believe that this GPCR is commonly used to promote cell activity in both vPN populations. From this finding, in insects, we can predict 5-HT7 expressing vPNs are the likely cell to be activated under low concentrations of 5-HT release to the circuit. Since this receptor has a stronger binding affinity to 5-HT, it could be used as a method to increase given cell activity within a circuit to allow for rapid neuron responses. If it is commonly expressed in our vPNs, is it also expressed in another sensory system with the same abundance?

The MCFO analysis also helped us understand the preferred glomeruli innervated by the vPNs. Generally, e-vPNs (expressing 5-HT1A, 1B, 2A, and 2B) innervated glomeruli tuned to attractive and aversive odors, while i-vPNs (5-HT7R) innervate generally attractive glomeruli but is capable of responding to aversive odors. Gathering information from both attractive and aversive stimuli is valuable for associated learning while responding to mostly attractive is important for rapid innate responses. This finding partially agrees with the finding from past research (Liang et al. 2013; Strutz et al. 2014) suggesting the roles of i-vPNs with innate attractive behaviors. The Liang paper describes that i-vPN provides parallel inhibition to vIPr neurons which reduces their responses to food odors but not pheromones while the Strutz model confirmed that the inhibition of vIPr neurons is used as a mechanism to the fly's attraction to innately attractive odors. Their findings are consistent with our results as the top 15 innervated glomeruli of the vPNs expressing 5-HTRs innervated attraction encoding glomeruli and a few aversive encoding glomeruli. Therefore, we suggest i-vPNs responding to aversive stimuli may be a result of odor discrimination done from providing inhibition in the presynaptic region ePN inputs innervating the AL (Parnas et al. 2013) or postsynaptic region contain LHN targets (Wang et al. 2014). This inhibition would better discrimination of given odors

Besides that, we found a glomerulus, VC2 that is innervated by all 5-HTR types and responds to all odor valence. It would be interesting to know more about how this neuropil contributes to the integration of odor types and how 5-HT modulation affects the synaptic environment of these glomeruli. The first step is to determine if the vPNs expressing a 5-HTR type have synaptic connections with the VC2 ORNs (Or71a) using GRASP. Then we can confirm if VC2 responds to both attractive (eugenol) and aversive odor (2-methylphenol). Then we could determine how a subpopulation that innervates VC2, R24H08 would behave when we manipulate its 5-HTR expression and respond to odors encoded by VC2. There are some analyses that could still be undertaken; 1) The likelihood of percent co-expression between receptor types and 2) a phylogenetic tree comparing the glomerular innervation patterns of

each type of 5-HTR expressing vPNs. We found out that some 5-HTR expressing vPNs in one population have similar exact percent glomerular innervation with each other, occurring multiple times in every other glomerulus. We wonder if the percent co-expression values are just coincidences or if these neurons are the same and is expressed in different 5-HTR populations. By creating a phylogenetic tree, we can infer which glomerular of a 5-HTR type is more similar to another, allowing us to determine co-expression from likelihood probabilities. We didn't explore too much of the LH due to complications interpreting innervation the patterns since i-vPNs are mostly expressed in 5-HT7.

In our next aim, we found two subpopulations of vPNs with two different 5-HTR expression profiles, the R24H08-LexA which expresses both 5-HT1AR and 5-HT1BR types while the R86G06-LexA expresses only the 5-HT7R. This is one of the best ways to study vPN subpopulations because 1) the vPN expressions can be controlled, 2) the populations are smaller than MZ699-Gal4 (Liang et al. 2013; Strutz et al. 2014), and 3) we could carry out other analyses such as determining their synaptic relationships, physiology, and role in mediating behavior. This method can be used to study both i-vPN and e-vPN populations, determining the similarities and differences in 5-HT modulation. Besides that, since we know that i-vPNs from the MZ699-Gal4 population respond to mostly attractive odor (Liang et al. 2013; Parnas et al. 2013; Strutz et al. 2014), we wanted to know if i-vPN are all GABAergic. Some confirmatory tests need to be done, especially on the R86G06 subpopulation which projects to the dorsal regions of the LH. A simple experiment is to confirm if R86G06 and R24H08 are GABAergic by analyzing their GABA contents. Next, we can determine if R86G06 and R24H08 are included in the MZ699-Gal4 subpopulation. Finally, we could remove expression in cholinergic neurons within our 5-HT7-T2A-Gal4 lines to see if any LH innervation patterns have similar innervations to the R86G06 line. This could be done by combining UAS-RFP, Aop-GFP-5-HTR-T2A-GAL4-MiMIC lines with ChAT-Gal80, which would allow us to visualize the expression of non-cholinergic vPN expression in the LH. Furthermore, a comparative connectome analysis needs to be done to understand the postsynaptic targets of the R86G06 driver lines and if there is any connectivity with the e-PN and e-vPN populations. Past studies indicated that 20% of the MZ699 vPNs are unlikely to GABAergic. It has been shown that the subset of innervations provide excitatory input to the dorsal regions, where e-PN and e-vPN reside (Shimizu and Stopfer 2017). Therefore, it is important to determine the neurotransmitter content of the R86G06 line to understand it's role in the LH.

To understand the LH, we need to know more about what LH neurons occupy the zones innervated by our vPNs. My first goal to understand the LH would be to create a 3-D layout of my LH innervations from the MCFO dataset (Refer Fig. 7F and 7G). This could be used to generate a heat map on where vPN expressing a 5-HTR type termination sites. We could also use sparse driver lines that only have the LH regions innervated by 5-HTR expressing vPNs. These two datasets help determine innervation patterns of 5-HTR expressing vPN innervation in the LH and identify their potential physiological effect in the LH zone based on what LH neurons they target. The first few steps of understanding 5-HT modulation in the LH is to classify the more specific zones where 5-HTR expressing vPNs can affect.

Lastly, with the subpopulation of neurons, we conduct behavioral assays to understand the effects of 5-HTR knockdown on odor-guided behavior. This comes after we demonstrated that a 5-HT1A receptor knockdown has increased attractive behavior to apple cider vinegar using the MZ699-Gal4 population (Ayad Auda's thesis, unpublished). We conducted this experiment on the R86G06-Gal4 population since no other neurons in this line express the 5-HT7 receptor. We saw a lot of variability with the T-maze assay with the odorant we worked with, 1-octen-3-ol across two different concentrations. Such variability could be caused by the genetics of the cross we worked with as well as the T-maze setup itself. Genetically, it could be that R86G06-Gal4 is only a small subpopulation of neurons that respond to 1-octen-3-ol out of a larger population. Next, the 5-HT7-RNAi could have a weaker effect in reducing the number of 5-HT7R within the subpopulation.

In terms of the setup itself, the flies were tested in a closed chamber with a volatile chamber. This could be an issue because the odorant has spread to all chambers of the T-maze before the fly has recovered from the cold shock, making the fly's final decision a 50/50 split. Next, the experiment only recorded the last position of the fly and not the activity of the fly's movement. This removes the information about fly activity during the behavior run and the exact time when all flies have made their decision. These factors mean that the T-maze assay does not holistically describe odor perception but the final odor choice.

We moved on to develop a fly arena assay based on a previous paper (Root et al. 2011), but the results were variable as well. The issue we ran with the fly arena assay was that we used one fly per run. We noticed that there was a lot of individuality in the fly's perception of 1-octen-3-ol. In future experiments, could use a total conditional silencing of the 5-HT7R vPNs in the fly's brain using temperature-sensitive UAS-shibire (van der Bliet and Meyerowitz 1991) combined with a teeshirt-Gal80 (Röder et al. 1992). Removing the activity of the whole population will allow us to know how much these specific vPNs affect responses to 1-octen-3-ol. This allows us to determine how much this population impacts odor-guided behavior. Adding a restricted t-shirt-Gal80 line (Röder et al. 1992) allows us to specifically target only the R86G06 neurons in the brain. On the other hand, we will be using a split-Gal4 line for our R24H08 driver line by removing expression coming from vIPr neurons found in the R24H08-Gal4. With that, we could understand the role of that i-vPN subpopulation toward farnesol. Farnesol is an attractive odorant found in citrus fruits that are carried into the DC3 glomerulus by Or83c (Ronderos et al. 2014). We chose this odorant for R24H08 split Gal4 because R24H08 vPNs innervate this glomerulus and strongly respond to the odor (Julius Jonaitis, unpublished).

In conclusion, I believe that behavioral assays and further analysis of the MCFO dataset should be the main focus of this project moving forward. Further analysis includes understanding if each similar glomerular innervation of each 5-HTR vPN is similar to each other and determining the LH innervation patterns of these 5-HTR expressing vPNs. This study has helped us understand the complexity and capability of 5-HT modulation within a set of projection neurons. Hopefully, the techniques and efforts of our findings will help us explore the workings of other 5-HT modulated regions within the brain as well as understand the advantages of having many neuromodulatory receptors within a sensory system.

References

- Ai M, Min S, Grosjean Y, Leblanc C, Bell R, Benton R, Suh GSB. 2010. Acid sensing by the *Drosophila* olfactory system. *Nature*. 468(7324):691–695. doi:10.1038/nature09537.
- Araki K, Nagata K. 2011. Protein Folding and Quality Control in the ER. *Cold Spring Harb Perspect Biol*. 3(11):a007526. doi:10.1101/cshperspect.a007526.
- Aso Y, Hattori D, Yu Y, Johnston RM, Iyer NA, Ngo T-T, Dionne H, Abbott L, Axel R, Tanimoto H, et al. 2014. The neuronal architecture of the mushroom body provides a logic for associative learning. Griffith LC, editor. *eLife*. 3:e04577. doi:10.7554/eLife.04577.
- Auda A. 2017 Jan 1. Serotonergic Modulation of Inhibitory Input to Lateral Horn Affects Odor-Mediated Attraction in *D. melanogaster*. Graduate Theses, Dissertations, and Problem Reports. doi:https://doi.org/10.33915/etd.5131. https://researchrepository.wvu.edu/etd/5131.
- Bargmann CI. 2012. Beyond the connectome: How neuromodulators shape neural circuits. *BioEssays*. 34(6):458–465. doi:10.1002/bies.201100185.
- Bates AS, Schlegel P, Roberts RJV, Drummond N, Tamimi IFM, Turnbull R, Zhao X, Marin EC, Popovici PD, Dhawan S, et al. 2020. Complete Connectomic Reconstruction of Olfactory Projection Neurons in the Fly Brain. *Curr Biol*. 30(16):3183-3199.e6. doi:10.1016/j.cub.2020.06.042.
- Becnel J, Johnson O, Luo J, Nässel DR, Nichols CD. 2011. The Serotonin 5-HT7Dro Receptor Is Expressed in the Brain of *Drosophila*, and Is Essential for Normal Courtship and Mating. *PLOS ONE*. 6(6):e20800. doi:10.1371/journal.pone.0020800.
- Berck ME, Khandelwal A, Claus L, Hernandez-Nunez L, Si G, Tabone CJ, Li F, Truman JW, Fetter RD, Louis M, et al. 2016. The wiring diagram of a glomerular olfactory system. Calabrese RL, editor. *eLife*. 5:e14859. doi:10.7554/eLife.14859.
- Berger M, Gray JA, Roth BL. 2009. The Expanded Biology of Serotonin. *Annual Review of Medicine*. 60(1):355–366. doi:10.1146/annurev.med.60.042307.110802.
- van der Blik AM, Meyerowitz EM. 1991. Dynamin-like protein encoded by the *Drosophila* shibire gene associated with vesicular traffic. *Nature*. 351(6325):411–414. doi:10.1038/351411a0.
- van Breugel F, Huda A, Dickinson MH. 2018. Distinct activity-gated pathways mediate attraction and aversion to CO₂ in *Drosophila*. *Nature*. 564(7736):420–424. doi:10.1038/s41586-018-0732-8.
- Bryson D, Qichen D, Chengcheng D, Charles S, Corbin J, Volkan Pelin C. 2021. Changes in splicing and neuromodulatory gene expression programs in sensory neurons with pheromone signaling and social experience. *Neuroscience*. [accessed 2022 Jun 18]. <http://biorxiv.org/lookup/doi/10.1101/2021.06.18.449021>.
- Chin SG, Maguire SE, Huoviala P, Jefferis GSXE, Potter CJ. 2018. Olfactory Neurons and Brain Centers Directing Oviposition Decisions in *Drosophila*. *Cell Reports*. 24(6):1667–1678. doi:10.1016/j.celrep.2018.07.018.

Coates KE, Calle-Schuler SA, Helmick LM, Knotts VL, Martik BN, Salman F, Warner LT, Valla SV, Bock DD, Dacks AM. 2020 Jul 8. The wiring logic of an identified serotonergic neuron that spans sensory networks. *J Neurosci*. doi:10.1523/JNEUROSCI.0552-20.2020. [accessed 2020 Jul 15].
<https://www.jneurosci.org/content/early/2020/07/08/JNEUROSCI.0552-20.2020>.

Coates KE, Majot AT, Zhang X, Michael CT, Spitzer SL, Gaudry Q, Dacks AM. 2017. Identified Serotonergic Modulatory Neurons Have Heterogeneous Synaptic Connectivity within the Olfactory System of *Drosophila*. *J Neurosci*. 37(31):7318–7331. doi:10.1523/JNEUROSCI.0192-17.2017.

Couto A, Alenius M, Dickson BJ. 2005. Molecular, anatomical, and functional organization of the *Drosophila* olfactory system. *Curr Biol*. 15(17):1535–1547. doi:10.1016/j.cub.2005.07.034.

Dacks AM, Christensen TA, Hildebrand JG. 2006. Phylogeny of a serotonin-immunoreactive neuron in the primary olfactory center of the insect brain. *Journal of Comparative Neurology*. 498(6):727–746. doi:<https://doi.org/10.1002/cne.21076>.

Dacks AM, Green DS, Root CM, Nighorn AJ, Wang JW. 2009. Serotonin Modulates Olfactory Processing in the Antennal Lobe of *Drosophila*. *J Neurogenet*. 23(4):366–377. doi:10.3109/01677060903085722.

Das Chakraborty S, Chang H, Hansson BS, Sachse S. 2022. Higher-order olfactory neurons in the lateral horn support odor valence and odor identity coding in *Drosophila*. Sen S, VijayRaghavan K, Sen S, Fiala A, editors. *eLife*. 11:e74637. doi:10.7554/eLife.74637.

Das Chakraborty S, Sachse S. 2021. Olfactory processing in the lateral horn of *Drosophila*. *Cell Tissue Res*. 383(1):113–123. doi:10.1007/s00441-020-03392-6.

Deng B, Li Q, Liu X, Cao Y, Li B, Qian Y, Xu R, Mao R, Zhou E, Zhang W, et al. 2019. Chemoconnectomics: Mapping Chemical Transmission in *Drosophila*. *Neuron*. 101(5):876-893.e4. doi:10.1016/j.neuron.2019.01.045.

Devineni AV, Scaplen KM. 2022. Neural Circuits Underlying Behavioral Flexibility: Insights From *Drosophila*. *Frontiers in Behavioral Neuroscience*. 15. [accessed 2022 Jun 26].
<https://www.frontiersin.org/article/10.3389/fnbeh.2021.821680>.

Devineni AV, Sun B, Zhukovskaya A, Axel R. Acetic acid activates distinct taste pathways in *Drosophila* to elicit opposing, state-dependent feeding responses. *eLife*. 8:e47677. doi:10.7554/eLife.47677.

Dolan M-J, Frechter S, Bates AS, Dan C, Huoviala P, Roberts RJ, Schlegel P, Dhawan S, Tabano R, Dionne H, et al. 2019. Neurogenetic dissection of the *Drosophila* lateral horn reveals major outputs, diverse behavioural functions, and interactions with the mushroom body. VijayRaghavan K, Grunwald Kadow IC, editors. *eLife*. 8:e43079. doi:10.7554/eLife.43079.

Drosophila external saline. 2011. *Cold Spring Harb Protoc*. 2011(9):pdb.rec065698. doi:10.1101/pdb.rec065698.

Ebrahim SAM, Dweck HKM, Stökl J, Hofferberth JE, Trona F, Weniger K, Rybak J, Seki Y, Stensmyr MC, Sachse S, et al. 2015. *Drosophila* Avoids Parasitoids by Sensing Their Semiochemicals via a Dedicated Olfactory Circuit. *PLOS Biology*. 13(12):e1002318. doi:10.1371/journal.pbio.1002318.

- Eid L, Champigny M-F, Parent A, Parent M. 2013. Quantitative and ultrastructural study of serotonin innervation of the globus pallidus in squirrel monkeys. *European Journal of Neuroscience*. 37(10):1659–1668. doi:10.1111/ejn.12164.
- Frechter S, Bates AS, Tootoonian S, Dolan M-J, Manton J, Jamasb AR, Kohl J, Bock D, Jefferis G. 2019. Functional and anatomical specificity in a higher olfactory centre. VijayRaghavan K, Grunwald Kadow IC, editors. *eLife*. 8:e44590. doi:10.7554/eLife.44590.
- Ganguly A, Qi C, Bajaj J, Lee D. 2020. Serotonin receptor 5-HT7 in *Drosophila* mushroom body neurons mediates larval appetitive olfactory learning. *Sci Rep*. 10(1):21267. doi:10.1038/s41598-020-77910-5.
- Gasque G, Conway S, Huang J, Rao Y, Vosshall LB. 2013. Small molecule drug screening in *Drosophila* identifies the 5HT2A receptor as a feeding modulation target. *Sci Rep*. 3(1):srep02120. doi:10.1038/srep02120.
- Getahun MN, Wicher D, Hansson BS, Olsson SB. 2012. Temporal response dynamics of *Drosophila* olfactory sensory neurons depends on receptor type and response polarity. *Front Cell Neurosci*. 6:54. doi:10.3389/fncel.2012.00054.
- Gnerer JP, Venken KJT, Dierick HA. 2015. Gene-specific cell labeling using MiMIC transposons. *Nucleic Acids Res*. 43(8):e56. doi:10.1093/nar/gkv113.
- Grabe V, Baschwitz A, Dweck HKM, Lavista-Llanos S, Hansson BS, Sachse S. 2016. Elucidating the Neuronal Architecture of Olfactory Glomeruli in the *Drosophila* Antennal Lobe. *Cell Reports*. 16(12):3401–3413. doi:10.1016/j.celrep.2016.08.063.
- Grabe V, Sachse S. 2018. Fundamental principles of the olfactory code. *Biosystems*. 164:94–101. doi:10.1016/j.biosystems.2017.10.010.
- Haq I ul, Cáceres C, Meza JS, Hendrichs J, Vreysen MJB. 2018. Different methods of methyl eugenol application enhance the mating success of male Oriental fruit fly (*Dipera*: Tephritidae). *Sci Rep*. 8(1):6033. doi:10.1038/s41598-018-24518-5.
- Heisenberg M. 2003. Mushroom body memoir: from maps to models. *Nat Rev Neurosci*. 4(4):266–275. doi:10.1038/nrn1074.
- Herrick-Davis K. 2013. Functional Significance of Serotonin Receptor Dimerization. *Exp Brain Res*. 230(4):375–386. doi:10.1007/s00221-013-3622-1.
- Hoffman ME. 1998. The Bull and the Silo: An Application of Curvature. *The American Mathematical Monthly*. 105(1):55–58. doi:10.2307/2589527.
- Huser A, Eschment M, Güllü N, Collins KAN, Böpple K, Pankevych L, Rolsing E, Thum AS. 2017. Anatomy and behavioral function of serotonin receptors in *Drosophila melanogaster* larvae. *PLoS One*. 12(8):e0181865. doi:10.1371/journal.pone.0181865.
- Inamdar AA, Hossain MM, Bernstein AI, Miller GW, Richardson JR, Bennett JW. 2013. Fungal-derived semiochemical 1-octen-3-ol disrupts dopamine packaging and causes neurodegeneration. *Proc Natl Acad Sci USA*. 110(48):19561–19566. doi:10.1073/pnas.1318830110.

Ito K, Shinomiya K, Ito M, Armstrong JD, Boyan G, Hartenstein V, Harzsch S, Heisenberg M, Homberg U, Jenett A, et al. 2014. A systematic nomenclature for the insect brain. *Neuron*. 81(4):755–765. doi:10.1016/j.neuron.2013.12.017.

Jeanne JM, Fişek M, Wilson RI. 2018. The Organization of Projections from Olfactory Glomeruli onto Higher-Order Neurons. *Neuron*. 98(6):1198-1213.e6. doi:10.1016/j.neuron.2018.05.011.

Jefferis GSXE, Potter CJ, Chan AM, Marin EC, Rohlfsing T, Maurer CR, Luo L. 2007. Comprehensive Maps of *Drosophila* Higher Olfactory Centers: Spatially Segregated Fruit and Pheromone Representation. *Cell*. 128(6):1187–1203. doi:10.1016/j.cell.2007.01.040.

Jenett A, Rubin GM, Ngo T-TB, Shepherd D, Murphy C, Dionne H, Pfeiffer BD, Cavallaro A, Hall D, Jeter J, et al. 2012. A GAL4-Driver Line Resource for *Drosophila* Neurobiology. *Cell Reports*. 2(4):991–1001. doi:10.1016/j.celrep.2012.09.011.

Johnson O, Becnel J, Nichols CD. 2009. Serotonin 5-HT₂ and 5-HT_{1A}-like receptors differentially modulate aggressive behaviors in *Drosophila melanogaster*. *Neuroscience*. 158(4):1292–1300. doi:10.1016/j.neuroscience.2008.10.055.

Jones WD, Cayirlioglu P, Grunwald Kadow I, Vosshall LB. 2007. Two chemosensory receptors together mediate carbon dioxide detection in *Drosophila*. *Nature*. 445(7123):86–90. doi:10.1038/nature05466.

Khallaf MA, Knaden M. 2022. Evolutionary neuroecology of olfactory-mediated sexual communication and host specialization in *Drosophila* – a review. *Entomologia Experimentalis et Applicata*. 170(4):289–302. doi:10.1111/eea.13143.

Kiebler MA, DesGroseillers L. 2000. Molecular Insights into mRNA Transport and Local Translation in the Mammalian Nervous System. *Neuron*. 25(1):19–28. doi:10.1016/S0896-6273(00)80868-5.

Knaden M, Strutz A, Ahsan J, Sachse S, Hansson BS. 2012. Spatial representation of odorant valence in an insect brain. *Cell Rep*. 1(4):392–399. doi:10.1016/j.celrep.2012.03.002.

Knecht ZA, Silbering AF, Cruz J, Yang L, Croset V, Benton R, Garrity PA. 2017. Ionotropic Receptor-dependent moist and dry cells control hygrosensation in *Drosophila*. Ramaswami M, editor. *eLife*. 6:e26654. doi:10.7554/eLife.26654.

Kurtovic A, Widmer A, Dickson BJ. 2007. A single class of olfactory neurons mediates behavioural responses to a *Drosophila* sex pheromone. *Nature*. 446(7135):542–546. doi:10.1038/nature05672.

Lai S-L, Awasaki T, Ito K, Lee T. 2008. Clonal analysis of *Drosophila* antennal lobe neurons: diverse neuronal architectures in the lateral neuroblast lineage. *Development*. 135(17):2883–2893. doi:10.1242/dev.024380.

Laissue P p., Reiter C, Hiesinger P r., Halter S, Fischbach K f., Stocker R f. 1999. Three-dimensional reconstruction of the antennal lobe in *Drosophila melanogaster*. *Journal of Comparative Neurology*. 405(4):543–552. doi:10.1002/(SICI)1096-9861(19990322)405:4<543::AID-CNE7>3.0.CO;2-A.

- Leng X, Wohl M, Ishii K, Nayak P, Asahina K. 2020. Quantifying influence of human choice on the automated detection of *Drosophila* behavior by a supervised machine learning algorithm. *PLoS One*. 15(12):e0241696. doi:10.1371/journal.pone.0241696.
- Li H, Horns F, Wu B, Xie Q, Li J, Li T, Luginbuhl DJ, Quake SR, Luo L. 2017. Classifying *Drosophila* Olfactory Projection Neuron Subtypes by Single-cell RNA Sequencing. *Cell*. 171(5):1206-1220.e22. doi:10.1016/j.cell.2017.10.019.
- Liang L, Li Y, Potter CJ, Yizhar O, Deisseroth K, Tsien RW, Luo L. 2013. GABAergic projection neurons route selective olfactory inputs to specific higher-order neurons. *Neuron*. 79(5):917-931. doi:10.1016/j.neuron.2013.06.014.
- Liang L, Luo L. 2010. The olfactory circuit of the fruit fly *Drosophila melanogaster*. *Sci China Life Sci*. 53(4):472-484. doi:10.1007/s11427-010-0099-z.
- Lobo FG, Bazargani M, Burke EK. 2020. A cutoff time strategy based on the coupon collector's problem. *European Journal of Operational Research*. 286(1):101-114. doi:10.1016/j.ejor.2020.03.027.
- Lone SR, Venkataraman A, Srivastava M, Potdar S, Sharma VK. 2015. Or47b-neurons promote male-mating success in *Drosophila*. *Biol Lett*. 11(5):20150292. doi:10.1098/rsbl.2015.0292.
- Luo M, Li Y, Zhong W. 2016. Do dorsal raphe 5-HT neurons encode "beneficialness"? *Neurobiology of Learning and Memory*. 135:40-49. doi:10.1016/j.nlm.2016.08.008.
- Lüscher C, Slesinger PA. 2010. Emerging roles for G protein-gated inwardly rectifying potassium (GIRK) channels in health and disease. *Nat Rev Neurosci*. 11(5):301-315. doi:10.1038/nrn2834.
- Mansourian S, Corcoran J, Enjin A, Löfstedt C, Dacke M, Stensmyr MC. 2016. Fecal-Derived Phenol Induces Egg-Laying Aversion in *Drosophila*. *Curr Biol*. 26(20):2762-2769. doi:10.1016/j.cub.2016.07.065.
- Marder E. 2012. Neuromodulation of Neuronal Circuits: Back to the Future. *Neuron*. 76(1):1-11. doi:10.1016/j.neuron.2012.09.010.
- Marder E, O'Leary T, Shruti S. 2014. Neuromodulation of Circuits with Variable Parameters: Single Neurons and Small Circuits Reveal Principles of State-Dependent and Robust Neuromodulation. *Annual Review of Neuroscience*. 37(1):329-346. doi:10.1146/annurev-neuro-071013-013958.
- Marin EC, Jefferis GSXE, Komiyama T, Zhu H, Luo L. 2002. Representation of the Glomerular Olfactory Map in the *Drosophila* Brain. *Cell*. 109(2):243-255. doi:10.1016/S0092-8674(02)00700-6.
- Maroteaux L, Béchade C, Roumier A. 2019. Dimers of serotonin receptors: Impact on ligand affinity and signaling. *Biochimie*. 161:23-33. doi:10.1016/j.biochi.2019.01.009.
- Min S, Ai M, Shin SA, Suh GSB. 2013. Dedicated olfactory neurons mediating attraction behavior to ammonia and amines in *Drosophila*. *Proc Natl Acad Sci U S A*. 110(14):E1321-1329. doi:10.1073/pnas.1215680110.
- Monti JM. 2011. Serotonin control of sleep-wake behavior. *Sleep Medicine Reviews*. 15(4):269-281. doi:10.1016/j.smr.2010.11.003.

- Münch D, Galizia CG. 2016. DoOR 2.0 - Comprehensive Mapping of *Drosophila melanogaster* Odorant Responses. *Sci Rep.* 6(1):21841. doi:10.1038/srep21841.
- Nern A, Pfeiffer BD, Rubin GM. 2015. Optimized tools for multicolor stochastic labeling reveal diverse stereotyped cell arrangements in the fly visual system. *PNAS.* 112(22):E2967–E2976. doi:10.1073/pnas.1506763112.
- Nichols DE, Nichols CD. 2008. Serotonin Receptors. *Chem Rev.* 108(5):1614–1641. doi:10.1021/cr078224o.
- Okada R, Awasaki T, Ito K. 2009. Gamma-aminobutyric acid (GABA)-mediated neural connections in the *Drosophila* antennal lobe. *Journal of Comparative Neurology.* 514(1):74–91. doi:10.1002/cne.21971.
- Olsen SR, Bhandawat V, Wilson RI. 2007. Excitatory Interactions between Olfactory Processing Channels in the *Drosophila* Antennal Lobe. *Neuron.* 54(1):89–103. doi:10.1016/j.neuron.2007.03.010.
- Olsen SR, Bhandawat V, Wilson RI. 2010. Divisive normalization in olfactory population codes. *Neuron.* 66(2):287–299. doi:10.1016/j.neuron.2010.04.009.
- Olsen SR, Wilson RI. 2008. Lateral presynaptic inhibition mediates gain control in an olfactory circuit. *Nature.* 452(7190):956–960. doi:10.1038/nature06864.
- Oram TB, Card GM. 2022. Context-dependent control of behavior in *Drosophila*. *Current Opinion in Neurobiology.* 73:102523. doi:10.1016/j.conb.2022.02.003.
- Parnas M, Lin AC, Huetteroth W, Miesenböck G. 2013. Odor Discrimination in *Drosophila*: From Neural Population Codes to Behavior. *Neuron.* 79(5):932–944. doi:10.1016/j.neuron.2013.08.006.
- Pfeiffer BD, Ngo T-TB, Hibbard KL, Murphy C, Jenett A, Truman JW, Rubin GM. 2010P. Refinement of Tools for Targeted Gene Expression in *Drosophila*. *Genetics.* 186(2):735–755. doi:10.1534/genetics.110.119917.
- Phelps JS, Hildebrand DGC, Graham BJ, Kuan AT, Thomas LA, Nguyen TM, Buhmann J, Azevedo AW, Sustar A, Agrawal S, et al. 2021. Reconstruction of motor control circuits in adult *Drosophila* using automated transmission electron microscopy. *Cell.* 184(3):759-774.e18. doi:10.1016/j.cell.2020.12.013.
- Prieto-Godino LL, Rytz R, Cruchet S, Bargeton B, Abuin L, Silbering AF, Ruta V, Dal Peraro M, Benton R. 2017. Evolution of Acid-Sensing Olfactory Circuits in *Drosophilids*. *Neuron.* 93(3):661-676.e6. doi:10.1016/j.neuron.2016.12.024.
- Racca C, Gardiol A, Triller A. 1998. Cell-specific dendritic localization of glycine receptor alpha subunit messenger RNAs. *Neuroscience.* 84(4):997–1012. doi:10.1016/s0306-4522(97)00585-x.
- Ren J, Friedmann D, Xiong J, Liu CD, Ferguson BR, Weerakkody T, DeLoach KE, Ran C, Pun A, Sun Y, et al. 2018. Anatomically Defined and Functionally Distinct Dorsal Raphe Serotonin Sub-systems. *Cell.* 175(2):472-487.e20. doi:10.1016/j.cell.2018.07.043.
- Renner U, Zeug A, Woehler A, Niebert M, Dityatev A, Dityateva G, Gorinski N, Guseva D, Abdel-Galil D, Fröhlich M, et al. 2012. Heterodimerization of serotonin receptors 5-HT1A and 5-HT7 differentially

- regulates receptor signalling and trafficking. *Journal of Cell Science*. 125(10):2486–2499. doi:10.1242/jcs.101337.
- Röder L, Vola C, Kerridge S. The role of the teashirt gene in trunk segmental identity in *Drosophila*. :19.
- Ronderos DS, Lin C-C, Potter CJ, Smith DP. 2014. Farnesol-Detecting Olfactory Neurons in *Drosophila*. *J Neurosci*. 34(11):3959–3968. doi:10.1523/JNEUROSCI.4582-13.2014.
- Root CM, Ko KI, Jafari A, Wang JW. 2011. Presynaptic Facilitation by Neuropeptide Signaling Mediates Odor-Driven Food Search. *Cell*. 145(1):133–144. doi:10.1016/j.cell.2011.02.008.
- Roskoski R. 2012. ERK1/2 MAP kinases: Structure, function, and regulation. *Pharmacological Research*. 66(2):105–143. doi:10.1016/j.phrs.2012.04.005.
- Roy B, Singh AP, Shetty C, Chaudhary V, North A, Landgraf M, VijayRaghavan K, Rodrigues V. 2007. Metamorphosis of an identified serotonergic neuron in the *Drosophila* olfactory system. *Neural Develop*. 2:20. doi:10.1186/1749-8104-2-20.
- Sakuma C, Anzo M, Miura M, Chihara T. 2014. Development of olfactory projection neuron dendrites that contribute to wiring specificity of the *Drosophila* olfactory circuit. *Genes Genet Syst*. 89(1):17–26. doi:10.1266/ggs.89.17.
- Sampson MM, Myers Gschweng KM, Hardcastle BJ, Bonanno SL, Sizemore TR, Arnold RC, Gao F, Dacks AM, Frye MA, Krantz DE. 2020. Serotonergic modulation of visual neurons in *Drosophila melanogaster*. Desplan C, editor. *PLoS Genet*. 16(8):e1009003. doi:10.1371/journal.pgen.1009003.
- Saudou F, Boschert U, Amlaiky N, Plassat JL, Hen R. 1992. A family of *Drosophila* serotonin receptors with distinct intracellular signalling properties and expression patterns. *EMBO J*. 11(1):7–17. doi:10.1002/j.1460-2075.1992.tb05021.x.
- Scheffer LK, Xu CS, Januszewski M, Lu Z, Takemura S, Hayworth KJ, Huang GB, Shinomiya K, Maitlin-Shepard J, Berg S, et al. 2020. A connectome and analysis of the adult *Drosophila* central brain. Marder E, Eisen MB, Pipkin J, Doe CQ, editors. *eLife*. 9:e57443. doi:10.7554/eLife.57443.
- Schultzhaus JN, Saleem S, Iftikhar H, Carney GE. 2017. The role of the *Drosophila* lateral horn in olfactory information processing and behavioral response. *Journal of Insect Physiology*. 98:29–37. doi:10.1016/j.jinsphys.2016.11.007.
- Semmelhack JL, Wang JW. 2009. Select *Drosophila* glomeruli mediate innate olfactory attraction and aversion. *Nature*. 459(7244):218–223. doi:10.1038/nature07983.
- Shimizu K, Stopfer M. 2017. A Population of Projection Neurons that Inhibits the Lateral Horn but Excites the Antennal Lobe through Chemical Synapses in *Drosophila*. *Frontiers in Neural Circuits*. 11. [accessed 2022 Jun 23]. <https://www.frontiersin.org/article/10.3389/fncir.2017.00030>.
- Silbering AF, Rytz R, Grosjean Y, Abuin L, Ramdya P, Jefferis GSXE, Benton R. 2011. Complementary Function and Integrated Wiring of the Evolutionarily Distinct *Drosophila* Olfactory Subsystems. *J Neurosci*. 31(38):13357–13375. doi:10.1523/JNEUROSCI.2360-11.2011.

- Sizemore TR, Dacks AM. 2016. Serotonergic Modulation Differentially Targets Distinct Network Elements within the Antennal Lobe of *Drosophila melanogaster*. *Scientific Reports*. 6:37119.
- Sizemore TR, Hurley LM, Dacks AM. 2020. Serotonergic modulation across sensory modalities. *Journal of Neurophysiology*. 123(6):2406–2425. doi:10.1152/jn.00034.2020.
- Stensmyr MC, Dweck HKM, Farhan A, Ibba I, Strutz A, Mukunda L, Linz J, Grabe V, Steck K, Lavista-Llanos S, et al. 2012. A Conserved Dedicated Olfactory Circuit for Detecting Harmful Microbes in *Drosophila*. *Cell*. 151(6):1345–1357. doi:10.1016/j.cell.2012.09.046.
- Strutz A, Soelster J, Baschwitz A, Farhan A, Grabe V, Rybak J, Knaden M, Schmuker M, Hansson BS, Sachse S. 2014. Decoding odor quality and intensity in the *Drosophila* brain. Ramaswami M, editor. *eLife*. 3:e04147. doi:10.7554/eLife.04147.
- Sweeney ST, Hidalgo A, Belle JS de, Keshishian H. 2011. Dissection of Adult *Drosophila* Brains. *Cold Spring Harb Protoc*. 2011(12):pdb.prot066878. doi:10.1101/pdb.prot066878.
- Tanaka NK, Endo K, Ito K. 2012. Organization of antennal lobe-associated neurons in adult *Drosophila melanogaster* brain. *J Comp Neurol*. 520(18):4067–4130. doi:10.1002/cne.23142.
- Task D, Lin C-C, Vulpe A, Afify A, Ballou S, Brbic M, Schlegel P, Raji J, Jefferis G, Li H, et al. 2022. Chemoreceptor co-expression in *Drosophila melanogaster* olfactory neurons. Grunwald Kadow IC, VijayRaghavan K, editors. *eLife*. 11:e72599. doi:10.7554/eLife.72599.
- Tierney AJ. 2018. Invertebrate serotonin receptors: a molecular perspective on classification and pharmacology. *Journal of Experimental Biology*. 221(19). doi:10.1242/jeb.184838. [accessed 2020 Dec 10]. <https://jeb.biologists.org/content/221/19/jeb184838>.
- Turner SL, Ray A. 2009. Modification of CO₂ avoidance behaviour in *Drosophila* by inhibitory odorants. *Nature*. 461(7261):277–281. doi:10.1038/nature08295.
- Vogt K, Zimmerman DM, Schlichting M, Hernandez-Nunez L, Qin S, Malacon K, Rosbash M, Pehlevan C, Cardona A, Samuel ADT. 2021. Internal state configures olfactory behavior and early sensory processing in *Drosophila* larvae. *Science Advances*. 7(1):eabd6900. doi:10.1126/sciadv.abd6900.
- Vosshall LB. 2000. Olfaction in *Drosophila*. *Current Opinion in Neurobiology*. 10(4):498–503. doi:10.1016/S0959-4388(00)00111-2.
- Vosshall LB, Stocker RF. 2007. Molecular architecture of smell and taste in *Drosophila*. *Annu Rev Neurosci*. 30:505–533. doi:10.1146/annurev.neuro.30.051606.094306.
- Wang K, Gong J, Wang Q, Li H, Cheng Q, Liu Y, Zeng S, Wang Z. 2014. Parallel pathways convey olfactory information with opposite polarities in *Drosophila*. *Proceedings of the National Academy of Sciences*. 111(8):3164–3169. doi:10.1073/pnas.1317911111.
- Wilson RI. 2013. Early Olfactory Processing in *Drosophila*: Mechanisms and Principles. *Annu Rev Neurosci*. 36:217–241. doi:10.1146/annurev-neuro-062111-150533.

Wong AM, Wang JW, Axel R. 2002. Spatial Representation of the Glomerular Map in the *Drosophila* Protocerebrum. *Cell*. 109(2):229–241. doi:10.1016/S0092-8674(02)00707-9.

Yasuyama K, Meinertzhagen IA, Schürmann F-W. 2003. Synaptic connections of cholinergic antennal lobe relay neurons innervating the lateral horn neuropile in the brain of *Drosophila melanogaster*. *Journal of Comparative Neurology*. 466(3):299–315. doi:10.1002/cne.10867.

Yu X, Ye Z, Houston CM, Zecharia AY, Ma Y, Zhang Z, Uygun DS, Parker S, Vyssotski AL, Yustos R, et al. 2015. Wakefulness Is Governed by GABA and Histamine Cotransmission. *Neuron*. 87(1):164–178. doi:10.1016/j.neuron.2015.06.003.

Zheng Z, Lauritzen JS, Perlman E, Robinson CG, Nichols M, Milkie D, Torrens O, Price J, Fisher CB, Sharifi N, et al. 2018. A Complete Electron Microscopy Volume of the Brain of Adult *Drosophila melanogaster*. *Cell*. 174(3):730-743.e22. doi:10.1016/j.cell.2018.06.019.

Ziegler AB, Berthelot-Grosjean M, Grosjean Y. 2013. The smell of love in *Drosophila*. *Front Physiol*. 4:72. doi:10.3389/fphys.2013.00072.